Factors Associated with the Downshear Reformation of Tropical Cyclones

Nathalie G. Rivera-Torres,[a] Kristen L Corbosiero,[a] Brian H. Tang[a]

[a] *Department of Atmospheric and Environmental Sciences, University at Albany, State University of New York, Albany, New York*

Corresponding author: Nathalie G. Rivera-Torres, nriveratorres@albany.edu

Early Online Release: This preliminary version has been accepted for publication in *Monthly Weather Review*, may be fully cited, and has been assigned DOI 10.1175/MWR-D-22-0251.1. The final typeset copyedited article will replace the EOR at the above DOI when it is published.

ABSTRACT

The conditions associated with tropical cyclones undergoing downshear reformation are explored for the North Atlantic basin from 1998 to 2020. These storms were compared to analog tropical cyclones with similar intensity, vertical wind shear, and maximum potential intensity, but did not undergo downshear reformation. Storm-centered, shear-relative composites were generated using ERA5 reanalysis and GridSat-B1 data. Downshear reformation predominately occurs for tropical cyclones of tropical storm intensity embedded in moderate vertical wind shear. A comparison between composites suggests that reformed storms are characterized by greater low-level and mid-tropospheric relative humidity downshear, larger surface latent heat fluxes downshear and left of shear, and larger low-level equivalent potential temperatures and CAPE right of shear. These factors increase thermodynamic favorability, building a reservoir of potential energy and decreasing dry air entrainment, promoting sustained convection downshear, and favoring the development of a new center.

SIGNIFICANCE STATEMENT

The development of a new low-level circulation center in tropical cyclones that replaces the original center, called downshear reformation, can affect the structure and intensity of storms, representing a challenge in forecasting tropical cyclones. While there have been a handful of case studies on downshear reformation, this study aims to more comprehensively understand the conditions that favor downshear reformation by comparing a large set of North Atlantic tropical cyclones that underwent reformation with a similar set of tropical cyclones that did not undergo reformation. Tropical cyclones that undergo reformation have a moister environment, larger surface evaporation, and higher low-level instability in specific regions that help sustain deep, downshear convection that favors the development of a new center.

1. Introduction

In tropical cyclones, downshear reformation is the process where a new low-level center develops within asymmetric convection downshear, replacing the parent vortex (Molinari et al. 2004). Center reformations can lead to abrupt changes in the structure and intensity of tropical cyclones, increasing forecast uncertainty. The cases of downshear reformation that have been documented in observational and modeling studies (Molinari et al. 2004, 2006; Davis et al. 2008; Chen et al. 2018b; Rogers et al. 2020; Alvey et al. 2022) had relatively weak intensity at the time of reformation (i.e., tropical depressions, tropical storms) and were in the early stages

Accepted for publication in *Monthly Weather Review*. DOI 10.1175/MWR-D-22-0251.1.

of their development. These case studies suggest that the reformation of tropical cyclones is more likely to occur in poorly defined, low-level circulations when they are more susceptible to inner-core processes and environmental factors than in well-organized, strong low-level circulations. Weaker tropical cyclones may be more susceptible than intense tropical cyclones due to their lower inertial stability and resistance to external forcings (Shapiro and Willoughby 1982) and because convection can more effectively reshape the rotational and irrotational velocity field (Schecter and Menelaou 2020).

The convective structure of tropical cyclones is influenced by vertical wind shear that induces an asymmetric secondary circulation and moisture distribution (Black et al. 2002; Chen et al. 2006; Rios-Berrios and Torn 2017). In sheared tropical cyclones, there is a preference for convection downshear (Corbosiero and Molinari 2002; Chen et al. 2006; Cecil 2007), although hurricane-strength sheared tropical cyclones are often characterized by a downshear-left precipitation maximum (Reasor et al. 2013; DeHart et al. 2014). The asymmetric vertical motion distribution in sheared tropical cyclones is generated by the thermal wind balance response to vertical wind shear acting to tilt the vortex downshear, displacing the center of circulation along a vertical axis due to differential vorticity advection (Jones 1995; DeMaria 1996). The strength of the vertical motion asymmetry increases with the vortex tilt (Jones 1995). Large and intense tropical cyclones are less susceptible to the effects of vertical wind shear (Jones 1995; DeMaria 1996; Reasor et al. 2004), but in immature or early-stage tropical cyclones, the vortex tilt can slow down the development of the tropical cyclone, prolonging the period of asymmetric convection far from the center (Schecter and Menelaou 2020; Yu et al. 2023).

The vortex tilt and asymmetries associated with the effects of vertical wind shear in tropical cyclones can affect the intensity and intensification by various mechanisms. When the vortex is tilted, the secondary circulation is less effective at converging absolute angular momentum inward to spin up the tangential wind (Riemer et al. 2010). In addition, the shear-induced tilt and asymmetries limit the axisymmetric projection of diabatic heating (Alvey et al. 2015) and transport low-entropy air downward, which can inhibit the intensification of tropical cyclones (Alland et al. 2021a,b) when the low-entropy parcels are not recovered by positive enthalpy fluxes (Tao and Zhang 2014; Chen et al. 2021b). Some tropical cyclones, however, have been documented to intensify, sometimes rapidly, in moderate to strong vertical wind shear after transitioning from a misaligned to an aligned structure (Rios-Berrios et al. 2016; Ryglicki et al. 2018; Alvey et al. 2020).

Accepted for publication in *Monthly Weather Review*. DOI 10.1175/MWR-D-22-0251.1.

Downshear reformation has been proposed as one mechanism for tropical cyclones to intensify under unfavorable environmental wind shear. Nguyen and Molinari (2015) found in simulations of Gabrielle (2001) that the relocation of the tropical cyclone center close to the downshear convection allowed diabatic heating to occur closer to the storm's center. The enhancement of diabatic heating closer to the center, in a region of high efficiency of kinetic energy production, was influential in Gabrielle's (2001) rapid intensification (Molinari and Vollaro 2010). The relocation of the low-level center can reduce the vortex tilt when the newly developed inner vortex, embedded in the broad envelope of cyclonic circulation associated with the parent vortex, is nearly upright and becomes the dominant vortex (Nguyen and Molinari 2015). Vortex tilt reduction because of reformation was also seen in Irene (2005), Vicente (2012), and Hermine (2016) (Davis et al. 2008; Chen et al. 2018b; Rogers et al. 2020). These cases rapidly intensified after the vortex tilt reduction. In Hermine (2016), the midlevel circulation showed a clear displacement from the low-level circulation. The evolution of the low- and mid-level centers suggested that Hermine (2016) achieved vertical alignment once the low-level center reformed underneath the midlevel center near deep convection and due to vorticity stretching (Rogers et al. 2020). The role of the midlevel center in early-stage tropical cyclone development has been previously examined and many cyclogenesis cases exhibit a midlevel vortex preceding the spin-up of an underlying low-level vortex (Raymond et al. 2014).

Previous work has described the adjustment of inner-core thermodynamic characteristics of tropical cyclones during their reformation. In Typhoon Vicente (2012) (Chen et al. 2019b), the inner-core thermodynamic state was characterized by an initially warm and dry layer in the lower-middle troposphere over the low-level circulation before reformation onset. Enhanced convective mixing, consistent with the increase of convective bursts associated with the reformation of the tropical cyclone and the vertical alignment, helped saturate the inner core in the lower-middle troposphere. Rogers et al. (2020) examined the evolution of the precipitation structure and the adjustment of the downshear thermodynamic environment of Hermine (2016), leading to the development of a low-level vortex. It was found that convection evolved from mostly deep to primarily moderate depth. The variation in the depth of convection was consistent with changes in the thermodynamic environment that evolved to be more moist and less unstable. The vertical mass flux profile transitioned to a bottom-heavy profile, resulting in stretching of vorticity in the lower troposphere. Similarly, Stone et al. (2023) found that the reformation of Sally (2020) was associated with low-level spin-up under a midlevel vortex as a result of the vertical stretching produced by the bottom-heavy mass flux, associated with

Accepted for publication in *Monthly Weather Review*. DOI 10.1175/MWR-D-22-0251.1.

small values of low- to midlevel moist convective instability and large column saturation fraction.

In an observational study of Danny (1997), Molinari et al. (2004) found that the development of an intense cell downshear, part of a series of shear-induced convective outbreaks, became the dominant vortex of the system. They hypothesized that the low-level center reformed near deep convection due to vorticity stretching. These results were supported by Molinari et al. (2006), where the reformation of Gabrielle (2001) was studied using observations. Like Danny (1997), Gabrielle (2001) was highly asymmetric and lacked convective activity near the center and upshear; after a significant convective outbreak downshear, a new circulation developed.

Numerical modeling studies have suggested that the persistent convection downshear that precedes reformation is associated with increased surface fluxes. In Nguyen and Molinari (2015), surface fluxes allowed moist entropy to increase downshear right, increasing the convective available potential energy (CAPE), which resulted in a favorable local environment to sustain intense convection downshear. In Chen et al. (2018b), elevated surface heat fluxes left of shear promoted the vigorous convective bursts that contributed to forming a strong mesovortex in a positive vorticity band. The high surface fluxes left of shear were related to the opposing directions of the vertical wind shear and background monsoon flow vectors. The location and role of anomalously large surface fluxes, particularly relative to the shear vector, in favoring downshear reformation requires further investigation.

Recently, Alvey et al. (2022) studied the reformation of Dorian (2019) and, in contrast to previous studies, the environment was characterized by decreasing shear at the time of reformation. Hours before the reformation, however, the system presented a shear-driven vortex misalignment and an asymmetric humidity distribution with dry air upshear that limited precipitation symmetry. Like other cases, a convective burst was observed before the reformation, allowing mesovortex-like features to develop and consolidate into the new vortex. In this case, it was hypothesized that island interaction invigorated the deep convective burst.

Until now, downshear reformation has been investigated only through case studies. A climatological analysis would provide more information about the environmental factors associated with downshear reformation in tropical cyclones to aid in forecasting. This study aims to identify the characteristics of reformed tropical cyclones that distinguish these systems from tropical cyclones with similar intensities and vertical wind shear that do not undergo downshear reformation using an analog approach. Section 2 describes the datasets employed

Accepted for publication in *Monthly Weather Review*. DOI 10.1175/MWR-D-22-0251.1.

in this study, the selection of cases, and a description of the analog method. Section 3 describes and compares the reformation and non-reformation composites, and section 4 gives the conclusions of this study.

2. Methodology and data

a. Domain

This study analyzes tropical cyclones in the North Atlantic basin from 1998 to 2020, based on the online availability of archived National Hurricane Center (NHC) discussions. Reformed tropical cyclones were identified from NHC discussions using keywords associated with downshear reformation (i.e., reformation, reforming, reformed, re-formed, reform, relocation, relocated, jog, jogged, jump, reposition, repositioning). Sub-tropical, extratropical, and tropical cyclones that reformed over land or made landfall within 12 h after reforming were excluded. Sixty tropical cyclones, making up the reformation (R) composite, were identified. Table 1, in Appendix A, contains all cases and the closest hour to the time of reformation in the NHC discussions. Additionally, as tropical cyclones may reform more than once during their lifetimes, the analysis focuses on the first reformation event.

It is not possible to objectively ascertain whether each case underwent downshear reformation. Nonetheless, the NHC discussions serve to identify plausible downshear reformation cases based on NHC Hurricane Specialists actively monitoring available data to track each TC center. A caveat to our methodology for identifying the cases is that it is not possible to know the exact time of reformation. There can be ambiguity as to whether the discussion refers to a reformation that happened prior to the time of writing or might be in the process of occurring.

b. Analog method

A list of tropical cyclones that did not go through reformation (NR) was generated using an analog method. Eligible non-reformation cases consisted of all other tropical cyclones during the study time period not listed in Table 1 as reformation cases (times where a non-reformation case was classified as sub-tropical, extratropical, or over land were excluded). The objective of the analog method is to identify, for each reformation case, a similar non-reformation case based on a set of chosen factors that may influence the reformation of tropical cyclones (Molinari et al. 2006). These factors are the maximum 10-m wind speed, deep-layer

Accepted for publication in *Monthly Weather Review*. DOI 10.1175/MWR-D-22-0251.1.

vertical wind shear, and maximum potential intensity. The analog selection attempts to control for these factors, producing analog pairs of similar intensity and in similar environments. In doing so, other potentially relevant factors differentiating reformation and non-reformation cases may be identified.

To objectively identify analogs, a cost function *J* (1) is defined, similar to Halperin and Torn (2018) and Richardson et al. (2022). The terms in *J* represent the normalized differences in the 850–200-hPa wind shear in a 200–800-km annulus from the center (*SHEAR*), maximum 10-m wind speed (*Vmax*), and maximum potential intensity (*MPI*). For the shear and maximum wind speed, differences are taken 12 h before the time of reformation for those cases and any eligible time for all non-reformation cases. For the MPI, differences are summed over a 24-h period, centered on the time of reformation for the reformation cases, and any contiguous 24-h period for all non-reformation cases. The 24-h period for the MPI requires analog TCs to be in similar thermodynamic environments for a sustained period. Differences are normalized by the variable's standard deviation (σ) for all eligible reformed and non-reformed tropical cyclones. *SHEAR* and *MPI* are extracted from the Statistical Hurricane Intensity Prediction Scheme (SHIPS) dataset (DeMaria and Kaplan 1994; DeMaria et al. 2005) and *Vmax* is the best track maximum wind (HURDAT2; Landsea and Franklin 2013). The data is available at 6-h time steps.

$$J = \left.\frac{|SHEAR_R - SHEAR_{NR}|}{\sigma_{SHR}}\right]_{t=-12} + \left.\frac{|Vmax_R - Vmax_{NR}|}{\sigma_{Vmax}}\right]_{t=-12} + \sum_{t=-12}^{12} \frac{|MPI_R - MPI_{NR}|}{\sigma_{MPI}} \quad (1)$$

The cost function was calculated for each reformation case and all eligible non-reformation cases and times. The non-reformation cases were then ranked in ascending order of the resultant cost function. The non-reformation case that minimized the value of *J* was selected as the best analog. If multiple reformation cases shared the same best analog, the non-reformation case was assigned to the reformation case for which the cost function was the lowest. The next available best analog was used for the remaining reformation cases to obtain unique analog pairs. Like Richardson et al. (2022), the analog pairs were retained when all

Accepted for publication in *Monthly Weather Review*. DOI 10.1175/MWR-D-22-0251.1.

terms of the cost function were ≤ 1.5 standard deviations from the term's mean to ensure the analogs were suitable matches. Figure 1 shows the distribution of each term on the right-hand side of (1), representing the normalized difference between each pair of analogs. The distribution indicates that MPI differences had the largest contribution to the total cost function, suggesting that the 24-h evolution of MPI was more challenging to match compared to the intensity and vertical wind shear.

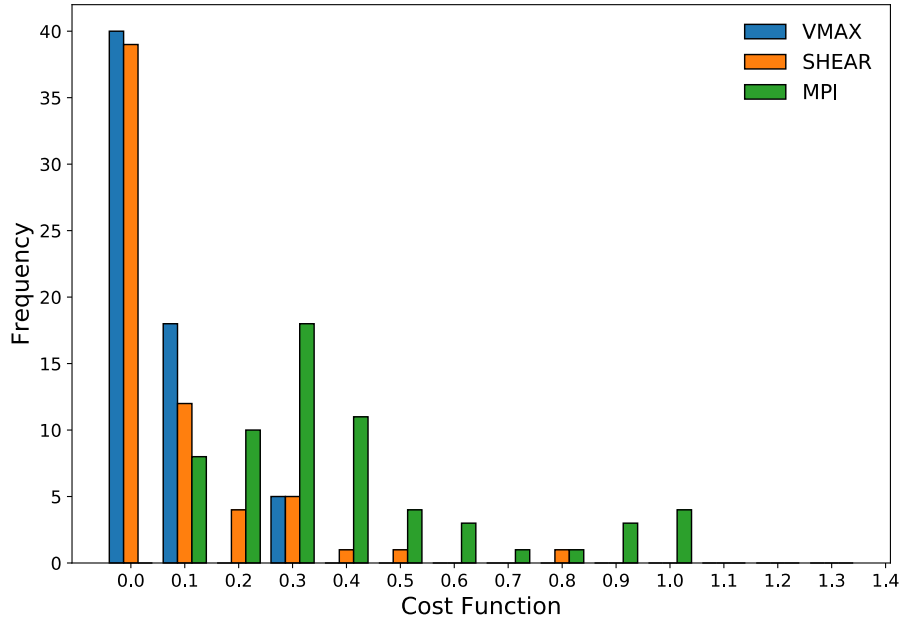

FIG. 1: Normalized difference in initial intensity (blue), initial vertical wind shear (orange), and maximum potential intensity (green) between analog reformation and non-reformation pairs.

Alternative cost functions were tested, such as one having the normalized difference in vertical wind shear summed over a 24-h period. However, this test resulted in higher values of *J*, and the magnitude of this term in the cost function exceeded the established threshold, reducing the number of good analog pairs. We settled on the current cost function based on simplicity and to maximize good analog matches.

A caveat to our methodology is that it is not possible to be certain that the non-reformation analog cases did not undergo reformation if the process was not observed or noted in NHC discussions. Nonetheless, the reformation cases have statistically significant larger 12-h forecast track and intensity error magnitudes compared to non-reformation cases (Figs. 2a and b). The larger track error may indicate unforecasted center jumps in the sample of reformation cases versus the sample of non-reformation cases. In addition, the forecast

Accepted for publication in *Monthly Weather Review*. DOI 10.1175/MWR-D-22-0251.1.

intensity error suggests an underprediction of the intensity (negative bias) of the reformed cases, possibly due to unexpected alignment. Figure 2 gives confidence that the method here distinguishes between reformation and non-reformation events.

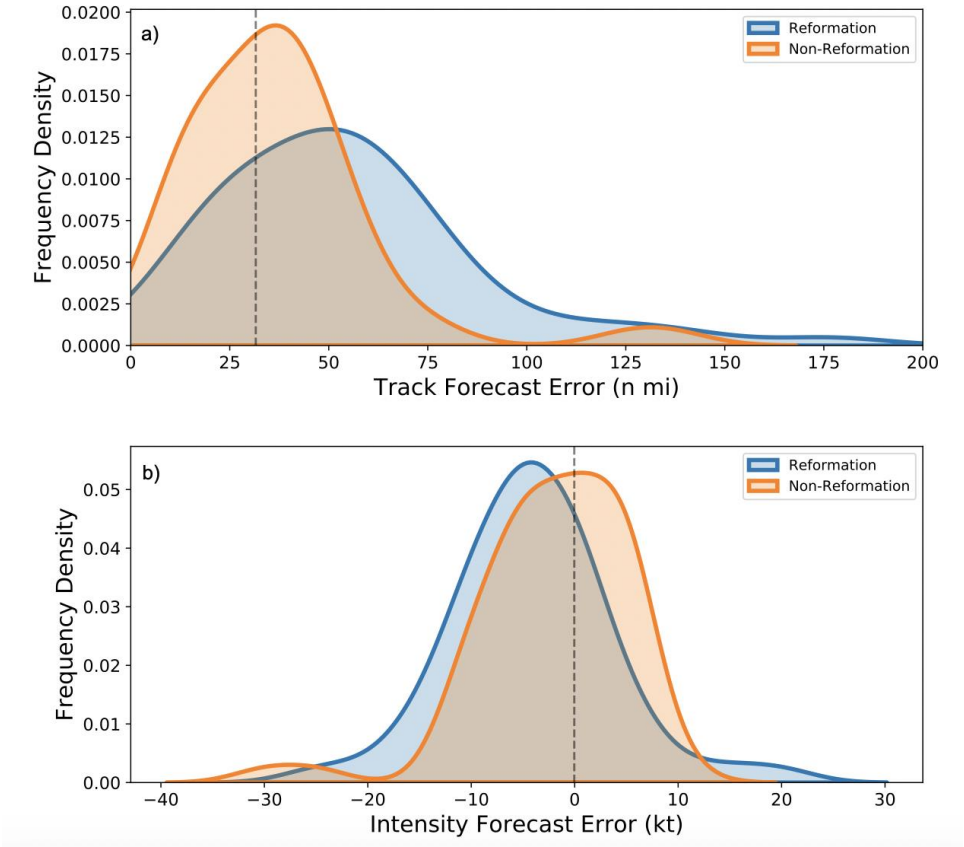

FIG. 2: (a) 12-h NHC track forecast error (n mi) for the reformation (blue) and non-reformation (orange) composites. The dashed line shows the mean value of the 12-h forecast track error for North Atlantic tropical cyclones from 1998–2020. b) Similar to (a) but for the intensity forecast error and mean bias (kt).

c. Datasets

Factors including relative humidity, equivalent potential temperature, CAPE, surface latent heat flux, wind speed, sea surface temperature, and mean sea level pressure were examined using the 5th-generation European Centre for Medium-Range Weather Forecasts (ECMWF) Reanalysis dataset (ERA5; Hersbach et al. 2020). This dataset provides hourly values of atmospheric and surface variables at 0.25ºx0.25º horizontal grid spacing. In addition, this study used Gridded Satellite infrared (IR) data from the International Satellite Cloud Climatology Project (ISCCP) dataset (GridSat-B1; Knapp et al. 2011). This dataset provides data from three channels with a grid spacing of 0.07º.

Accepted for publication in *Monthly Weather Review*. DOI 10.1175/MWR-D-22-0251.1.

Data were examined using storm-centered composites rotated relative to the vertical wind shear direction. The latter was done due to vertical wind shear's strong influence on structural asymmetries in tropical cyclones (e.g., Nguyen et al. 2019). Like Fischer et al. (2019), the location of a tropical cyclone's center was determined by calculating the 850-hPa relative vorticity centroid from the ERA5 dataset within a 3ºx3º box centered in the best track position. This method corrects for instances in which there are deviations from the best track position due to the coarse resolution of the reanalysis dataset. The tropical cyclone's center position may not, however, represent the new center's location, as ERA5 likely does not resolve the reformation. The shear direction used to rotate the composites was extracted from the SHIPS dataset.

d. Low-level mean flow

Similar to Chen et al. (2021), the low-level mean flow was defined as the 850-hPa mean flow. The mean flow at that height was calculated following the tropical cyclone vortex removal method described in Galarneau and Davis (2013), where the rotational and divergent components of the wind were subtracted from the wind field within a 500-km radius from the tropical cyclone center. Once the tropical cyclone vortex was removed, the mean flow was the average wind field within 500 km.

e. Statistical significance testing

Differences between analog tropical cyclone fields were computed, composited, and tested for statistical significance at the 95% confidence interval using a bootstrap resampling approach similar to Rios-Berrios et al. (2016) and Richardson et al. (2022). The first step of this approach was generating two subsets of 63 members randomly sampled with replacements from the combined reformation and non-reformation cases. Then, the differences between the two subsets were computed. These two steps were repeated 1000 times to create the null distribution used to test the null hypothesis. The null hypothesis is that the composite difference between the reformation and non-reformation cases is statistically indistinguishable from the composite difference between two randomly generated groups.

3. Results and discussion

a. Climatological characteristics

Accepted for publication in *Monthly Weather Review*. DOI 10.1175/MWR-D-22-0251.1.

Since most case studies of downshear reformation are tropical storms under moderate vertical wind shear at the time, or prior to the time, of reformation (e.g., Nguyen and Molinari 2015; Chen et al. 2018; Rogers et al. 2020), we first examined the magnitudes of the maximum 10-m wind speed and vertical wind shear. Hereafter, we will refer to the reformation time and the analog match time as t = 0 h and perform composite analyses about these times.

Figure 3 shows intensity distributions from t=-12 h to t=0 h for the reformation and non-reformation cases. The intensity at t=-12 h ranged from 25–55 kt (e.g., tropical depression to tropical storm intensity) for both composites. The difference between composites was not statistically significant at the 95% confidence interval, which is expected as the -12-h intensity was controlled for in the analog cost function. Over time, the intensity distributions shifted to stronger wind speeds, but the systems mostly stayed as tropical storms and depressions. At the time of reformation, 97% of the cases were tropical storms, consistent with the sample of reformation cases that have been documented in observational and modeling studies (Molinari et al. 2004, 2006; Davis et al. 2008; Chen et al. 2018b; Rogers et al. 2020; Alvey et al. 2022; Alvey and Hazelton 2022). Although most tropical cyclones remained as tropical storms from -6 to 0 h in both composites, the reformation composite had a larger mean intensity increase. After the reformation, seven reformed tropical cyclones rapidly intensified, while in the non-reformation composite, three tropical cyclones rapidly intensified (RI $\geq$ 25 kt in 24 h; Kaplan et al. 2010); however, there was no statistically significant difference in the 24-h intensity change between composites. The different intensity changes outcomes suggest that there is not a definite relationship between reformation and intensity change.

Accepted for publication in *Monthly Weather Review*. DOI 10.1175/MWR-D-22-0251.1.

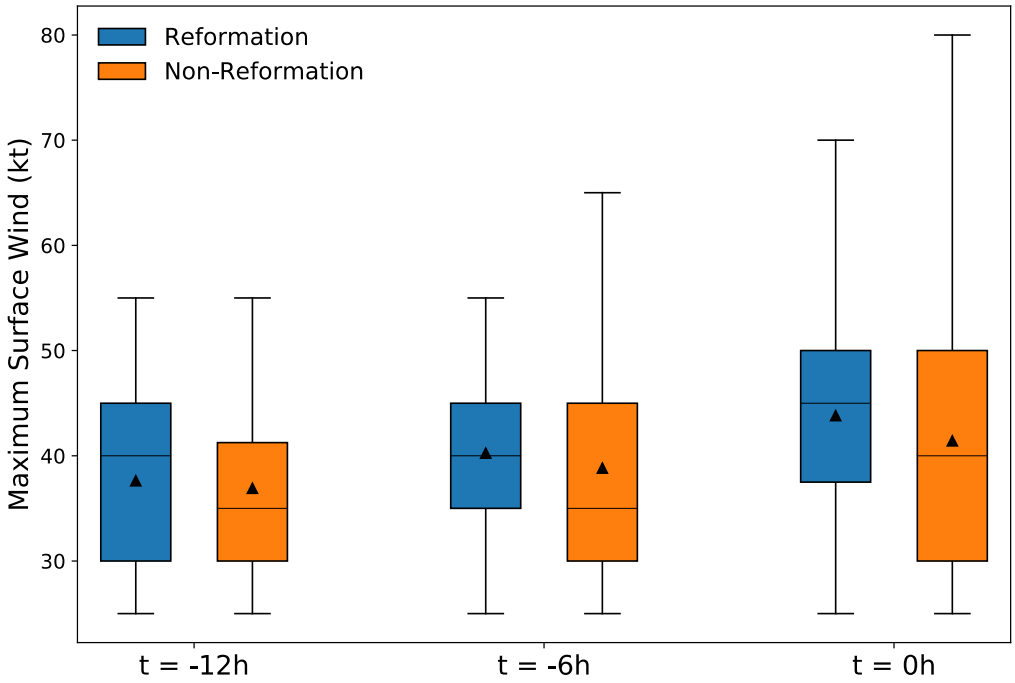

FIG. 3. Intensity (kt) box plots at t = -12, -6, and 0 h for reformation cases (blue), and the non-reformation cases (orange). Whiskers extend from the minimum to the maximum and boxes extend from the 25th to the 75th percentiles. The median is marked by the line dividing the boxes and the triangles represent the distribution's mean.

The 850–200-hPa shear magnitude distributions at t = -12 h, -6 h, and 0 h are shown in Figure 4. The distributions were broad, with shear ranging from weak to strong. At t= -12 h, the reformation and non-reformation distributions had an interquartile range mostly in the moderate vertical wind shear range (4.5–11.0 m s^{-1}; Rios-Berrios and Torn 2017) with means around 7.5 m s^{-1}. At -6 and 0 h, the mean and median shear remained around 7.5–8.5 m s^{-1}. Differences between the distributions at all times were not statistically significant.

Accepted for publication in *Monthly Weather Review*. DOI 10.1175/MWR-D-22-0251.1.

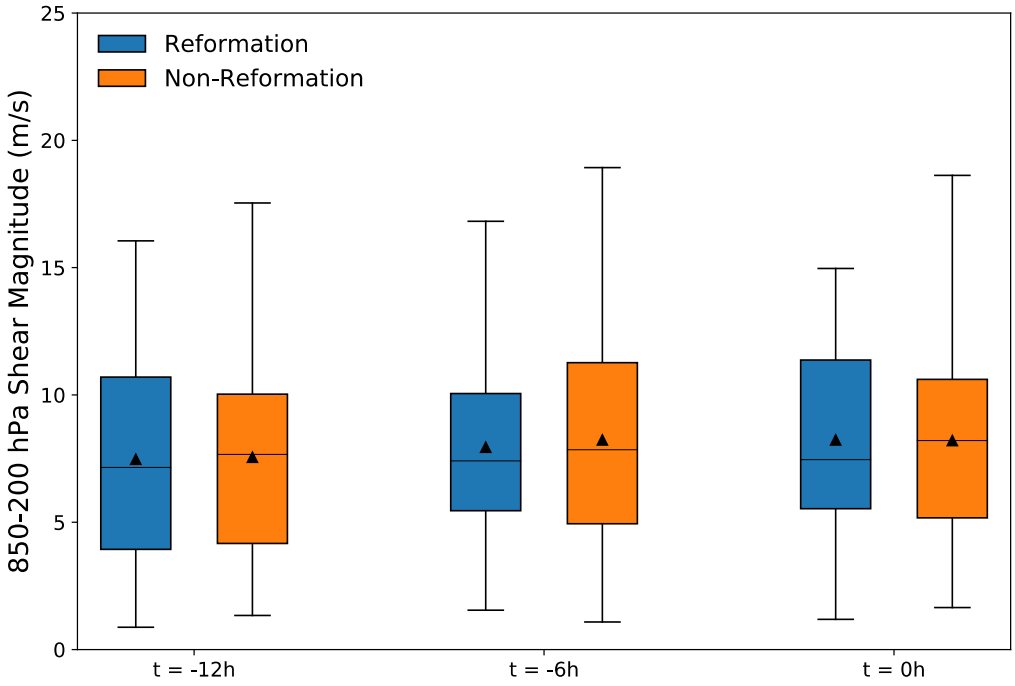

FIG. 4. Similar to Fig. 2, except for the 850–200-hPa shear magnitude (m s^{-1}) at t = -12, -6, and 0 h for reformation cases (blue) and non-reformation cases (orange).

Figure 5 shows the normalized distributions of cyclone age, defined as the hours between the time a system was classified as a tropical cyclone by the NHC and the estimated time of reformation for reformation cases or the analog match time for non-reformation cases. Focusing on the age distribution of the reformation cases, the distribution peaked at 28 h and the likelihood of reformation decreased with age. This result suggests that reformation is more likely during the early stages of a system. The mean and median of the age distribution of the reformed tropical cyclones was larger. Although the age distribution of the non-reformation cases had a similar distribution peak, it was even more concentrated in the early stages of a system's lifetime. The Mann–Whitney U test showed no statistically significant difference between the age distributions. Thus, the comparison that follows is predominantly tropical cyclones within a few days after genesis (i.e., of a similar age), a desirable outcome of the analog method.

Accepted for publication in *Monthly Weather Review*. DOI 10.1175/MWR-D-22-0251.1.

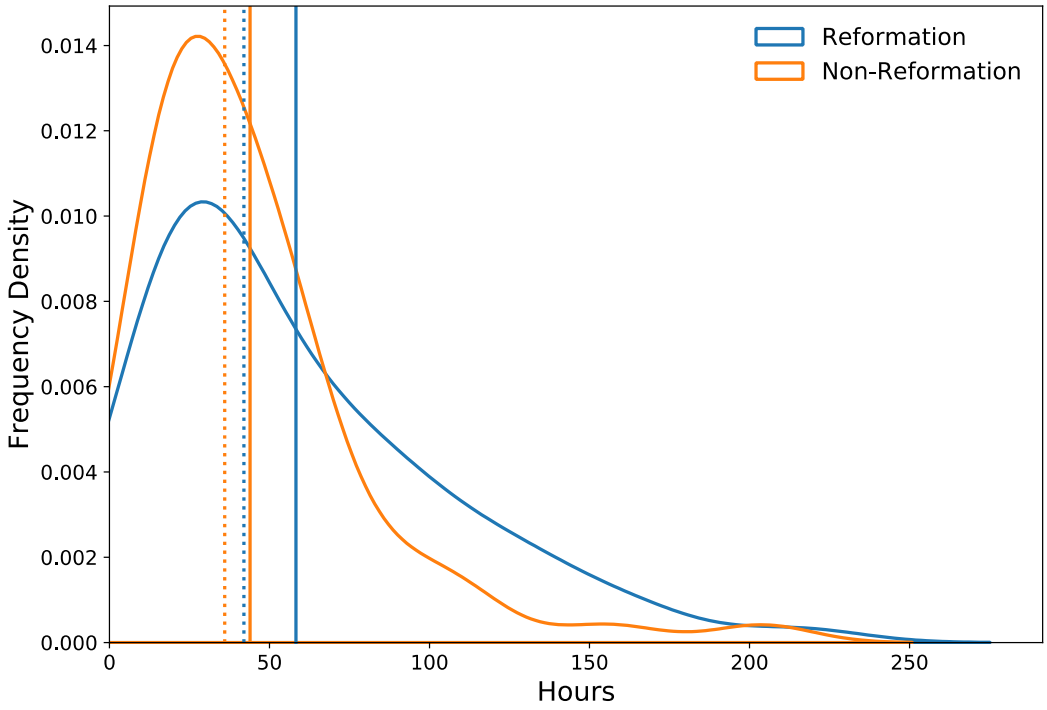

FIG. 5. Normalized distribution of tropical cyclone age for reformation cases (blue) and analog non-reformation cases (orange). The solid lines give the mean of the distributions and the dotted lines are the median of the distributions.

The location of the reformation cases at the time of reformation and the analog non-reformation cases are shown in Figure 6. Each group had a similar geographic distribution across the basin, except in the eastern Atlantic (< 40° W) where there were fewer reformation cases. Clusters of reformation cases are also evident in the Gulf of Mexico and the western Caribbean Sea.

Accepted for publication in *Monthly Weather Review*. DOI 10.1175/MWR-D-22-0251.1.

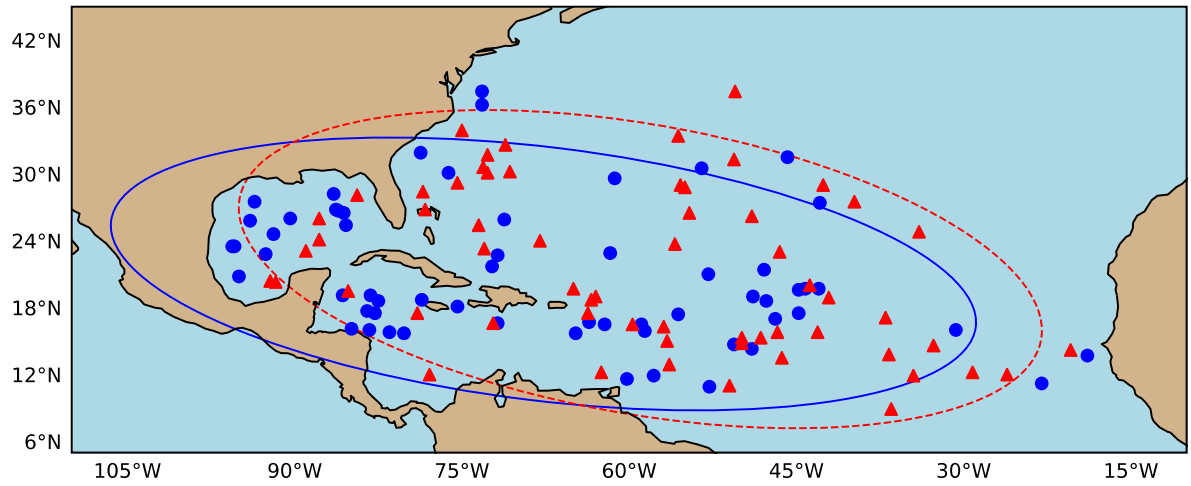

FIG. 6. Location of the reformation cases (blue circles) and analog non-reformation cases (red triangles). The blue (solid) ellipse encloses the reformation distribution centroids at 2σ counts and the red (dashed) ellipse is from the non-reformation distribution.

b. Thermodynamic environmental characteristics

Differences in tropospheric relative humidity were investigated between tropical cyclones that reformed versus those that did not. Storm-centered, shear-relative, composite-mean lower-tropospheric (850–700-hPa layer average) and mid-tropospheric (500–300-hPa layer average) relative humidity are shown in Figures 7 and 8, respectively. During -12–0 h, the reformation composite had greater lower-tropospheric relative humidity than the non-reformation composite. The mid-tropospheric relative humidity was asymmetric, with higher humidity downshear and lower relative humidity upshear. These asymmetries could be the result of vertical shear-induced tilted circulations with enhanced upward motion downshear and subsidence upshear. Molinari et al. (2006) found a similar asymmetric distribution of relative humidity before the reformation of Gabrielle (2001), with air subsiding as it moved cyclonically towards the upshear quadrants.

The difference between the reformation and non-reformation composites showed that reformed storms had statistically significant larger relative humidity directly downshear. The area of positive difference moved inward from -12 to 0 h due to an inward increase in relative humidity in the reformed storms and a decrease in relative humidity in the non-reformed storms. The increase seemed to be associated with the relative humidity physically increasing and not a shift in the center position, as the reanalysis data and/or the tropical cyclone center finding technique was not able to capture the jump in the center position caused by the reformation. Upshear, however, the reformed storms had smaller relative humidity values that

Accepted for publication in *Monthly Weather Review*. DOI 10.1175/MWR-D-22-0251.1.

could inhibit convection. Examining the specific humidity for both composites (not shown), the same distribution as the relative humidity fields existed, with larger values in the downshear region for the reformation composite.

The comparison suggests that reformed tropical cyclones are in a moister low-tropospheric environment and have a more asymmetric azimuthal moisture distribution at mid-levels with larger relative humidity downshear and smaller relative humidity upshear. The differences in relative humidity indicate the importance of the moisture content in the reformation of tropical cyclones. These results are consistent with previous observations of reformed tropical cyclones (Molinari et al. 2006; Molinari and Vollaro 2010; Rogers et al. 2020; Alvey et al. 2022). The smaller relative humidity in the lower and middle troposphere, particularly downshear, in the non-reformation composite, suggests greater inhibition of convective activity, which will be examined in a subsequent subsection.

Accepted for publication in *Monthly Weather Review*. DOI 10.1175/MWR-D-22-0251.1.

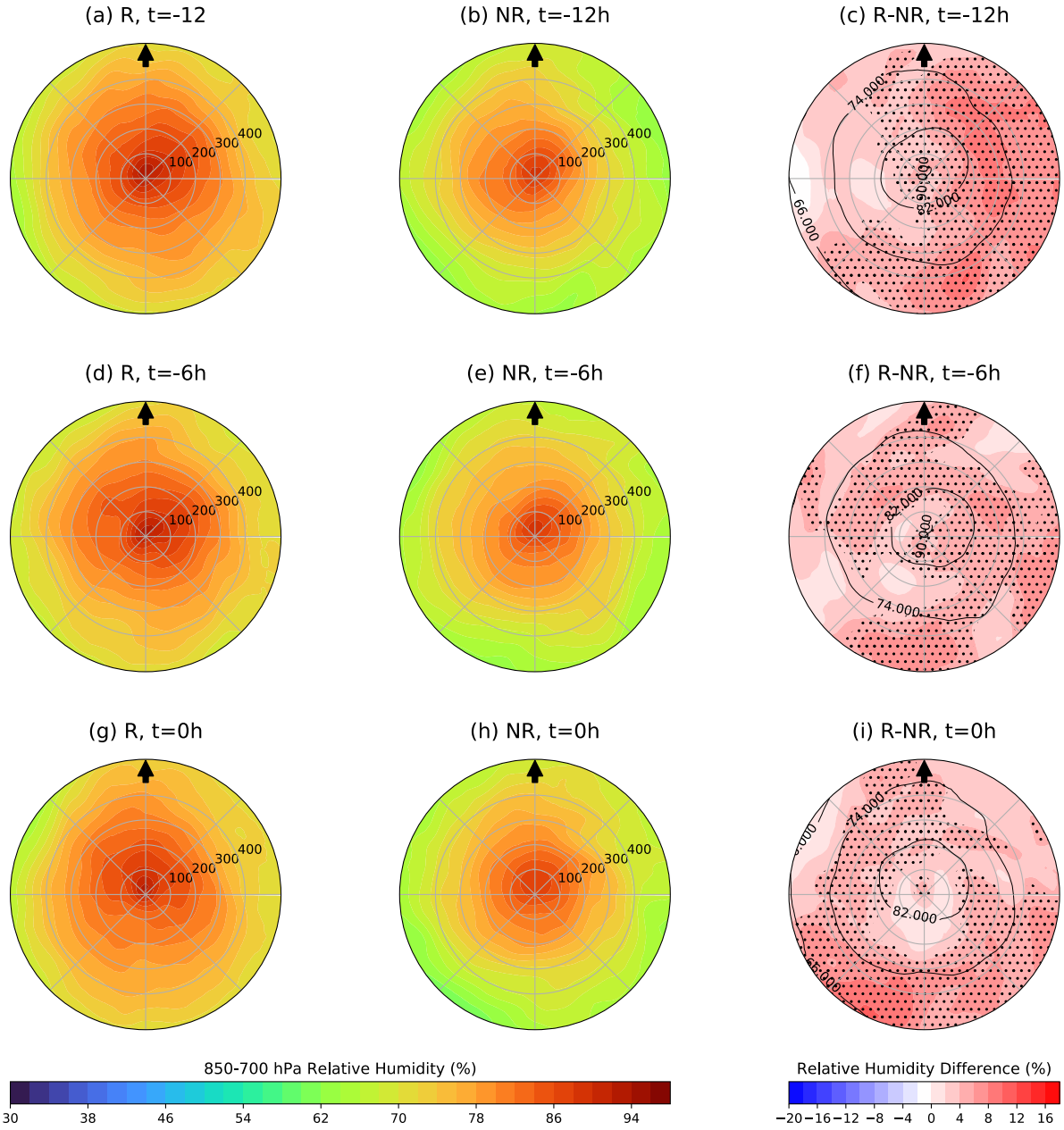

FIG. 7. Composite-mean, storm-centered, shear-relative, 850–700-hPa relative humidity (%) for (a) the reformation composite, (b) the non-reformation composite, and (c) the difference between the two composites at -12 h; (d)–(f) and (g)–(i) as in (a)–(c), but at -6 h and 0 h, respectively. Composites are rotated by the 850–200-hPa wind shear direction given by the black arrow. In (c), (f), and (i), contours represent the all-sample mean and the stippling denotes where the differences are statistically significant at the 95% confidence level. The radius of each circle is in kilometers (km).

Accepted for publication in *Monthly Weather Review*. DOI 10.1175/MWR-D-22-0251.1.

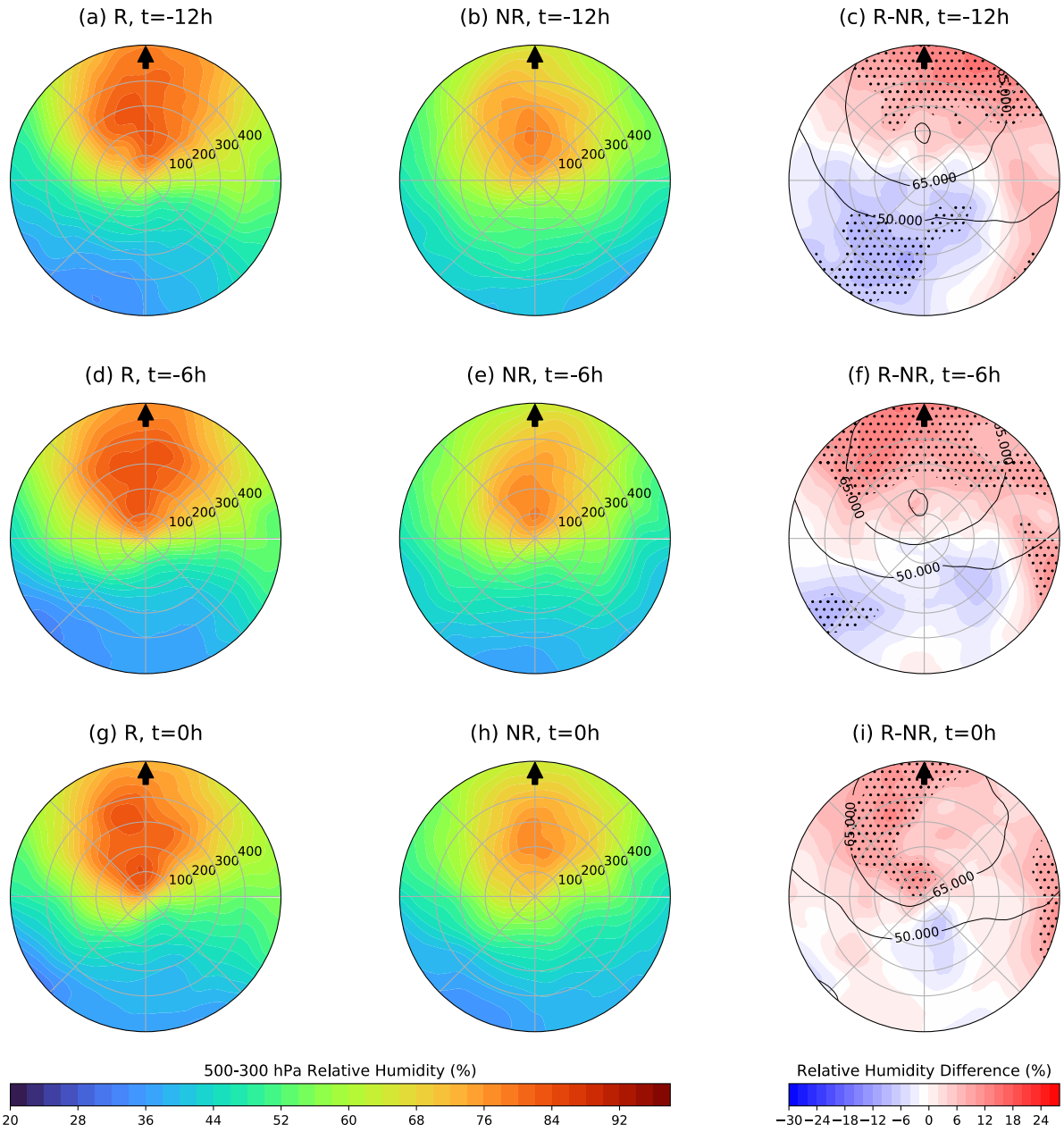

FIG. 8. Similar to Fig. 7, but for the 500–300-hPa relative humidity (%).

As asymmetric convection in sheared tropical cyclones might be associated with low-level thermodynamic asymmetries (Zhang et al. 2013), differences in low-level moist entropy were examined. Figure 9 shows the composite means and differences in 1000-hPa equivalent potential temperature (θ_e). During -12 h–0 h, the reformation composite had higher θ_e right of shear, nearly 3 K higher than left of shear. This pattern differed from the azimuthal distribution of θ_e in the non-reformation composite, where θ_e was more uniform within 400 km. The higher values of θ_e right of shear in the reformed storms were statistically significant, suggesting that this region of higher θ_e was favorable for the reformation of tropical cyclones. At 400 hPa, θ_e

Accepted for publication in *Monthly Weather Review*. DOI 10.1175/MWR-D-22-0251.1.

was asymmetric, with the highest values in the downshear quadrants for both composites (not shown). Compared to the non-reformation composite, the reformation composite had statistically significantly higher midlevel θ_e in the downshear region, consistent with mid-level moistening there.

The low-level θ_e asymmetry in the reformation composite, with lower values left of shear, is consistent with the results of Nguyen and Molinari (2015); however, their θ_e maxima were found in the downshear-right quadrant, similar to Zhang et al. (2013). In this study, the reformed composite had the maxima in the upshear-right quadrant. This difference could be associated with the coarse resolution of the reanalysis data, as their composite examined the inner-core region using dropsonde data. Nonetheless, the high θ_e right of shear in the reformation composite represented an increased reservoir of energy to sustain convection downshear that was much more muted in the non-reformation composite.

To assess the difference in the potential instability available for convection between the reformation and non-reformation cases, most-unstable CAPE was compared (Fig. 10). Consistent with Molinari et al. (2012), CAPE increased away from the center and there was higher CAPE downshear relative to upshear. Compared to Fig. 9, these differences were more spatially variable and had less statistically significant area. At t=0 h, the CAPE difference was generally consistent with the θ_e difference, suggesting more instability right of shear to fuel downshear convection in reformed storms, consistent with Alvey and Hazelton (2022).

Accepted for publication in *Monthly Weather Review*. DOI 10.1175/MWR-D-22-0251.1.

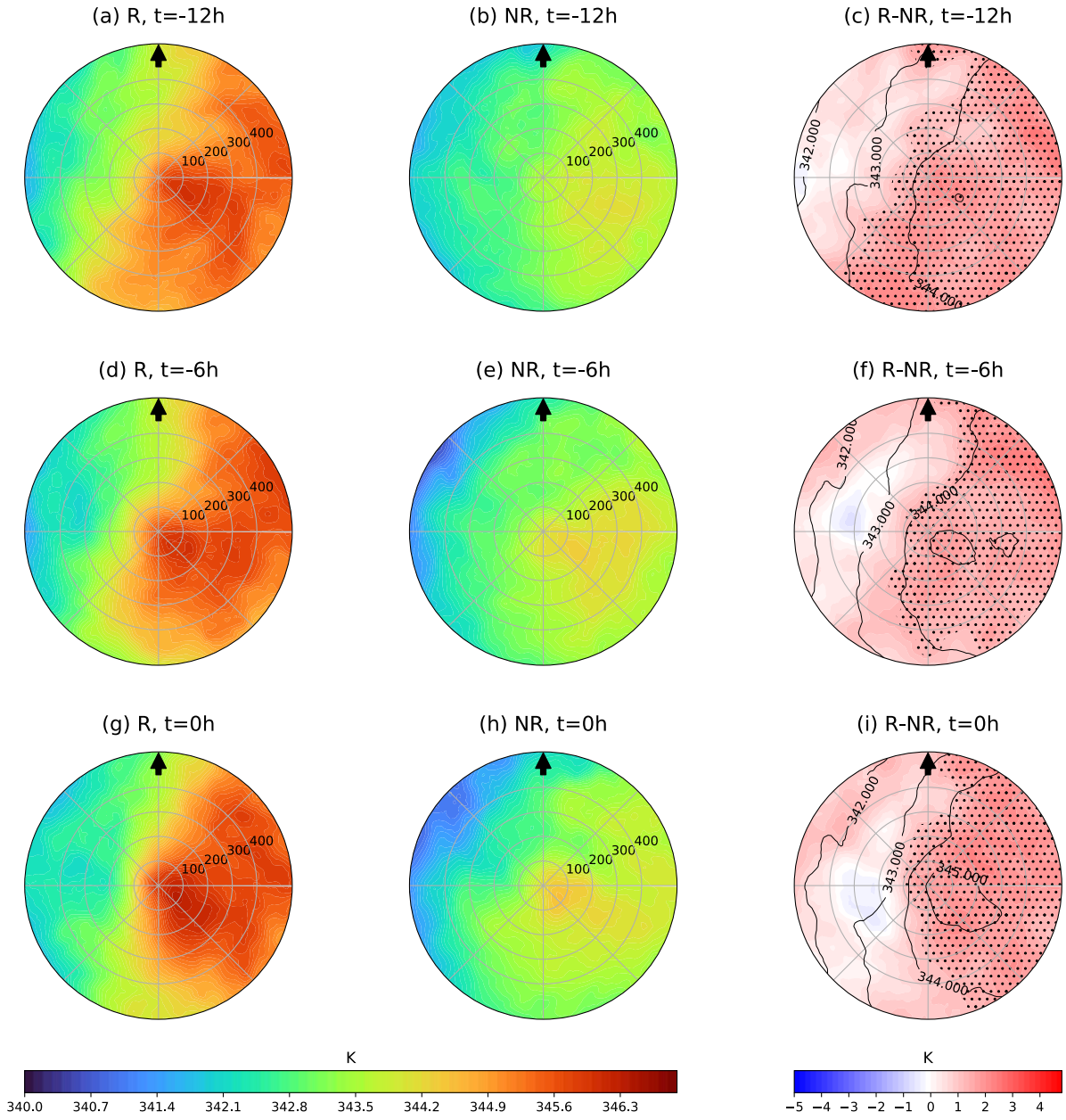

FIG. 9. Similar to Fig. 7, except for the 1000-hPa equivalent potential temperature (K).

Accepted for publication in *Monthly Weather Review*. DOI 10.1175/MWR-D-22-0251.1.

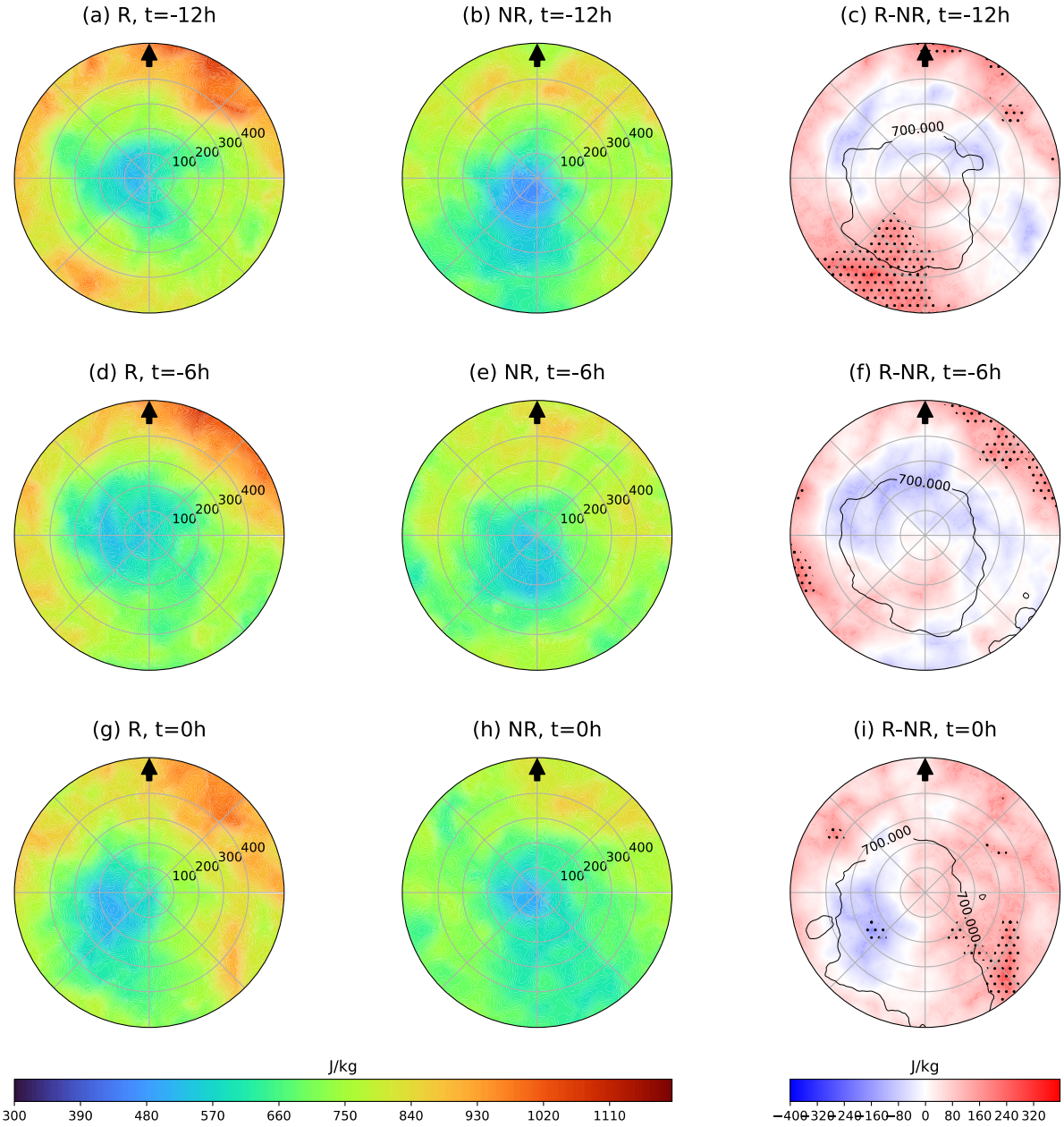

FIG. 10. Similar to Fig. 7, except for the CAPE (J kg^{-1}).

c. Surface fluxes

The differences in θ_e and CAPE motivate a comparison of surface latent heat fluxes between reformation and non-reformation cases. Figure 11 shows the composite-mean surface latent heat flux for the reformation and non-reformation composites, and their differences. Both composites showed an asymmetric surface latent heat flux distribution, with maximum values generally left of shear. From -12 to 0 h, the surface latent heat flux increased notably in the reformation composite. In contrast, the surface latent heat fluxes increased slightly in the non-reformation composite. The composite differences showed that reformed tropical cyclones had

Accepted for publication in *Monthly Weather Review*. DOI 10.1175/MWR-D-22-0251.1.

statistically significant higher fluxes downshear and left of shear within 400 km from the center. Hence, the larger and increasing surface latent heat fluxes downshear and left of shear were a distinguishing characteristic between the reformation and non-reformation storms. The larger values of surface fluxes left of shear in the reformation composite could explain the increase in θ_e right of shear, as the surface fluxes could boost the moist entropy as seen in previous studies (Rappin and Nolan 2012; Chen et al. 2019a).

The increase of the left-of-shear surface heat fluxes is consistent with Chen et al. (2018b), where an increase in surface latent fluxes downshear left was associated with an increase of convective bursts that led to Typhoon Vicente's (2012) reformation. In their study, the increase in latent heat fluxes was due to the increase in surface wind speed left of shear. The increase in surface wind speed resulted from the superposition of the low-level southwesterly monsoon flow, in a direction opposite to the environmental wind shear, on the tropical cyclone circulation. As the tropical cyclone circulation intensified, the surface latent heat flux gradually amplified.

Motivated by this finding, the role of the orientation of the low-level wind and vertical wind shear directions was examined. The angle between the vertical wind shear and the low-level mean flow vector was calculated counterclockwise from the shear vector. For example, a low-level mean flow directly left of shear would result in an angle of 90º. Figure 12 shows the distribution of the angle between the vertical wind shear vector and low-level mean flow direction for both composites. The mean angle between the shear vector and low-level mean flow direction was 115º for the reformation distribution and 148º for the non-reformation distribution. Both angles indicate that the low-level mean flow was left of shear, with the reformation composite having a distribution more peaked to the left of shear than the non-reformation distribution. The difference in the orientation of the low-level flow relative to shear between the two composites was statistically significant using the bootstrap resampling approach. Left-of-shear directed low-level flow increases surface fluxes downshear, i.e., to the right of the low-level flow vector, because of the superposition of the cyclonic flow and the background flow. The increase in the surface fluxes in the reformation composite, therefore, could also be associated with the orientation of the low-level flow relative to shear. Previous studies have documented that left-of-shear, low-level mean flow induces asymmetries in the surface wind field with stronger winds and positive surface flux anomalies mostly downshear left (Chen et al. 2018a, 2019a, 2021a).

Accepted for publication in *Monthly Weather Review*. DOI 10.1175/MWR-D-22-0251.1.

To assess if the surface latent heat flux differences between reformation and non-reformation cases were associated with surface wind speed differences, Figure 13 shows the composite-mean 10-m wind speed. Maximum surface winds were lower than the best track values, likely due to the coarse resolution of the reanalysis data; however, the patterns in Fig. 13 were similar to those in Figure 11. The reformation cases had stronger surface winds downshear and left of shear than the non-reformation cases. Additionally, the reformation cases had a more pronounced downshear left increase in wind speed from -12 to 0 h compared to the non-reformation cases. This result suggests that the increase in surface latent heat flux was linked to the increase in surface wind speed.

Accepted for publication in *Monthly Weather Review*. DOI 10.1175/MWR-D-22-0251.1.

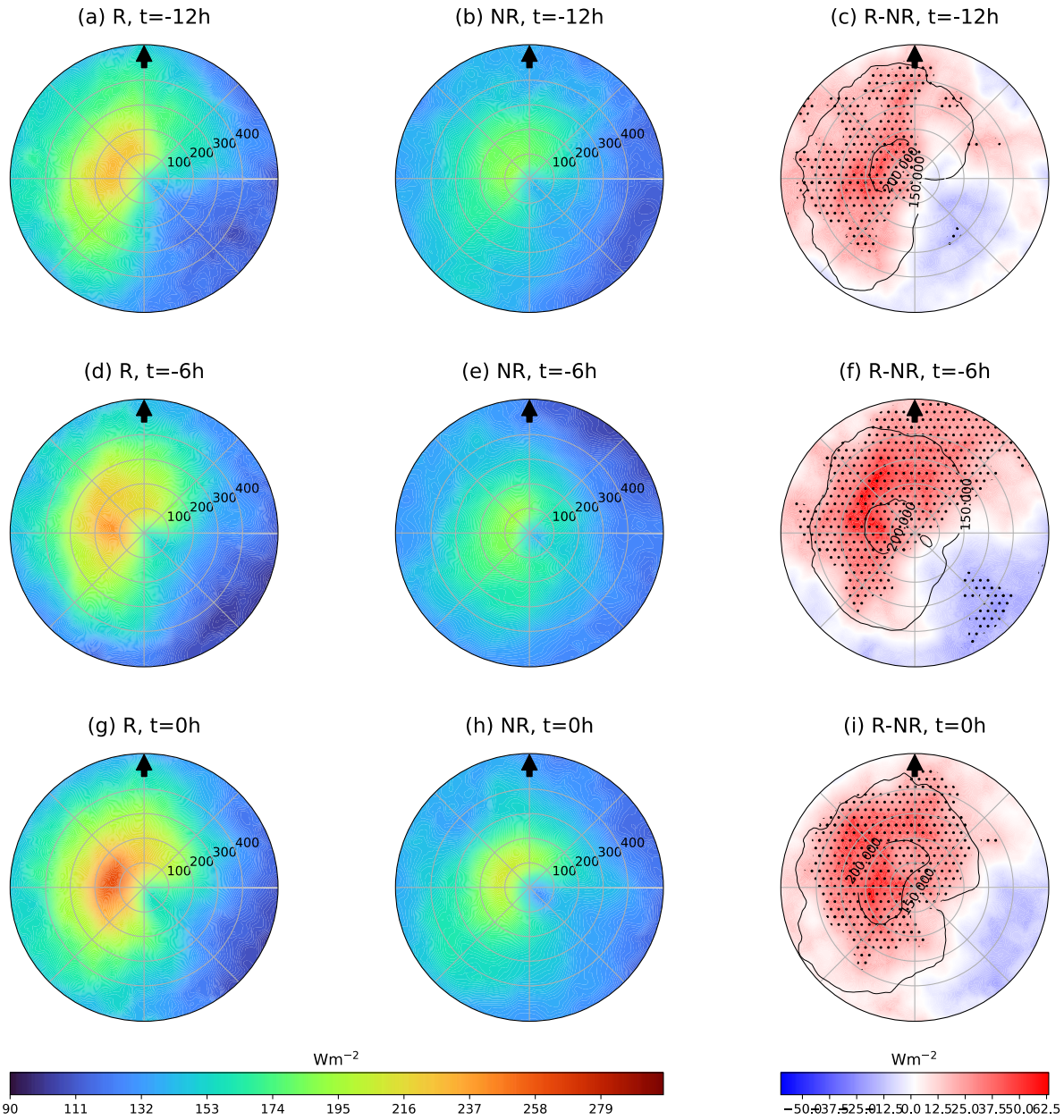

FIG. 11. Similar to Fig. 7, except for the surface latent heat flux (W m^{-2}).

Accepted for publication in *Monthly Weather Review*. DOI 10.1175/MWR-D-22-0251.1.

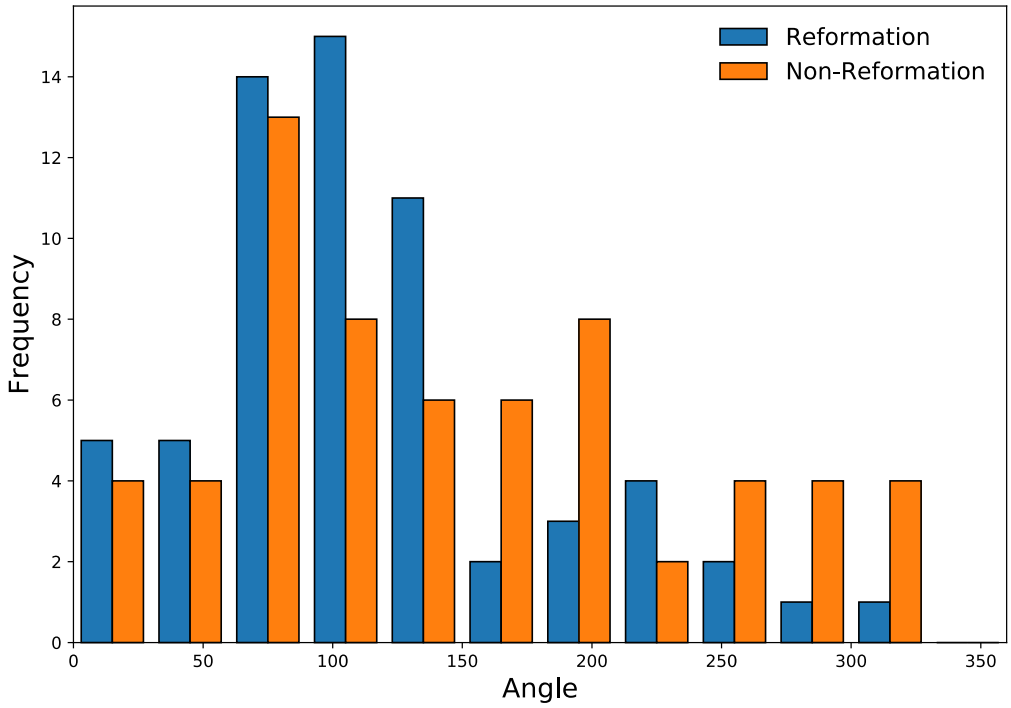

FIG. 12. Distribution of the angle between vertical wind shear and low-level mean flow (°) at t = 0 h for reformation cases (blue) and non-reformation cases (orange).

The mean sea level pressure (MSLP) was examined to further assess the causes of the larger wind speed downshear and left of shear in the reformation composite (Fig. 14). Both the reformation and non-reformation composites had an asymmetric MSLP distribution, with the highest values downshear left and the lowest values upshear right. Compared to the non-reformation composite, the reformation composite had lower MSLP near the center, but similar MSLP downshear left. The result was a stronger pressure gradient in the reformation composite coinciding with the area of larger 10-m wind speeds noted in Fig. 13.

Accepted for publication in *Monthly Weather Review*. DOI 10.1175/MWR-D-22-0251.1.

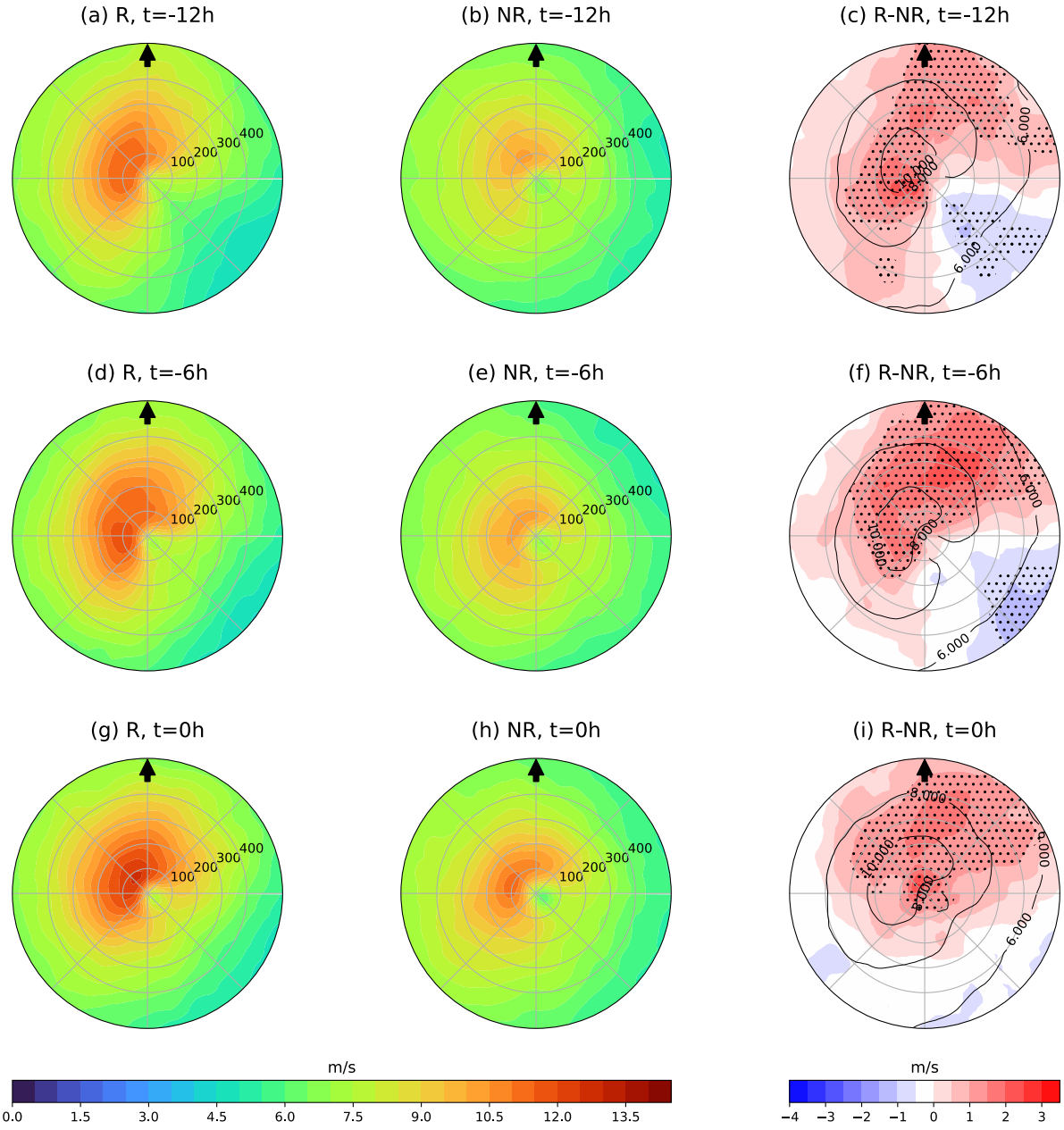

FIG. 13. Similar to Fig. 7, except for the 10-m wind speed (m s^{-1}).

Interestingly, reformation cases had lower MSLP in the upshear-right quadrant extending to >800 km, which possibly reflected differences in the background environment in which reformation and non-reformation cases were embedded. Examination of individual reformation cases that had lower upshear-right MSLP showed that these cases were primarily located in the Caribbean and the Gulf of Mexico. In addition, two reformation cases right off the west coast of Africa showed a similar pattern in the MSLP distribution. The lower MSLP seemed to reflect a larger, synoptic-scale, trough-like feature that the tropical cyclone was embedded in (not shown), much like Typhoon Vicente's interaction with a monsoon circulation

Accepted for publication in *Monthly Weather Review*. DOI 10.1175/MWR-D-22-0251.1.

(Chen et al. 2018b). Interactions of tropical cyclones with low-level, trough-like features are one possible factor in downshear reformation that was not further investigated in this study but would be an interesting follow-on topic to explore.

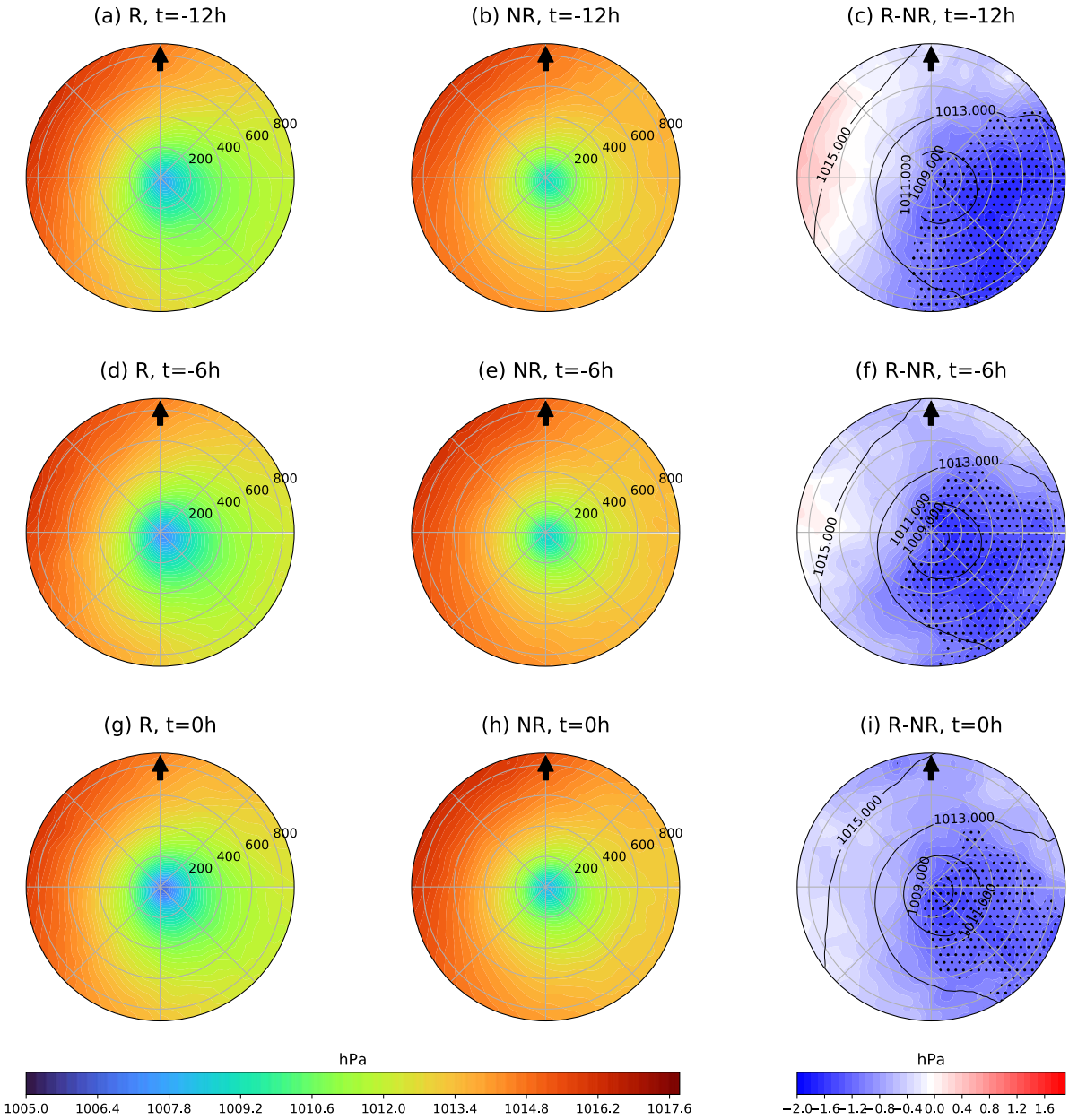

FIG. 14. Similar to Fig. 7, except for the mean sea level pressure (hPa). Note the larger radius in these plots to capture more of the environment.

d. Convective characteristics

To complement the ERA5-based analysis, the spatial and temporal distribution of the convective activity of the reformation and non-reformation composites was examined using

Accepted for publication in *Monthly Weather Review*. DOI 10.1175/MWR-D-22-0251.1.

infrared (IR) brightness temperature (Fig. 15). In both composites, the coldest IR brightness temperatures were displaced downshear, as one would expect (e.g., Corbosiero and Molinari 2002), although averaging the brightness temperature in the composites likely removed any signal of the most intense convection. At -12 h, the reformed storms had an area of deep convection (<228 K; Wang 2018) downshear within 100 km from the center. Over the following six hours, cloud tops cooled and expanded downshear. Approaching the time of reformation, the cloud tops continued to cool downshear. In contrast, non-reformation cases showed little change in the coldest IR brightness temperature between -12 and -6 h. Perhaps importantly, the coldest IR brightness temperatures at -6 h were closer to the center, compared to the reformation cases, which would help amplify the primary vortex versus any competing vortex downshear. In the reformation composite, the coldest brightness temperatures maximized between 100–200 km downshear, which would support reformation. As a result, the most negative differences in IR brightness temperature between reformed and non-reformed storms were downshear at -6 h. The overall IR brightness temperature tendencies and differences suggest that sustained, deepening convection downshear is a characteristic of reformed tropical cyclones, consistent with observational studies of downshear reformation (Molinari et al. 2006; Alvey et al. 2022).

e. Subsample sensitivity

Given that there are some differences in the geographic distribution between reformation and non-reformation cases (Fig. 6), we performed subsampling of the full sample of reformation and non-reformation cases and repeated the composite analysis above. For example, we formed a subsample of cases only located in the Gulf of Mexico and the western Caribbean and a subsample of cases excluding cases in the eastern Atlantic. For some fields and subsamples, there are small azimuthal shifts in the composite difference fields, along with changes in difference magnitudes, which we attribute to a reduction in sample size (not shown). The main findings of this study, however, remain consistent for these different subsamples.

Accepted for publication in *Monthly Weather Review*. DOI 10.1175/MWR-D-22-0251.1.

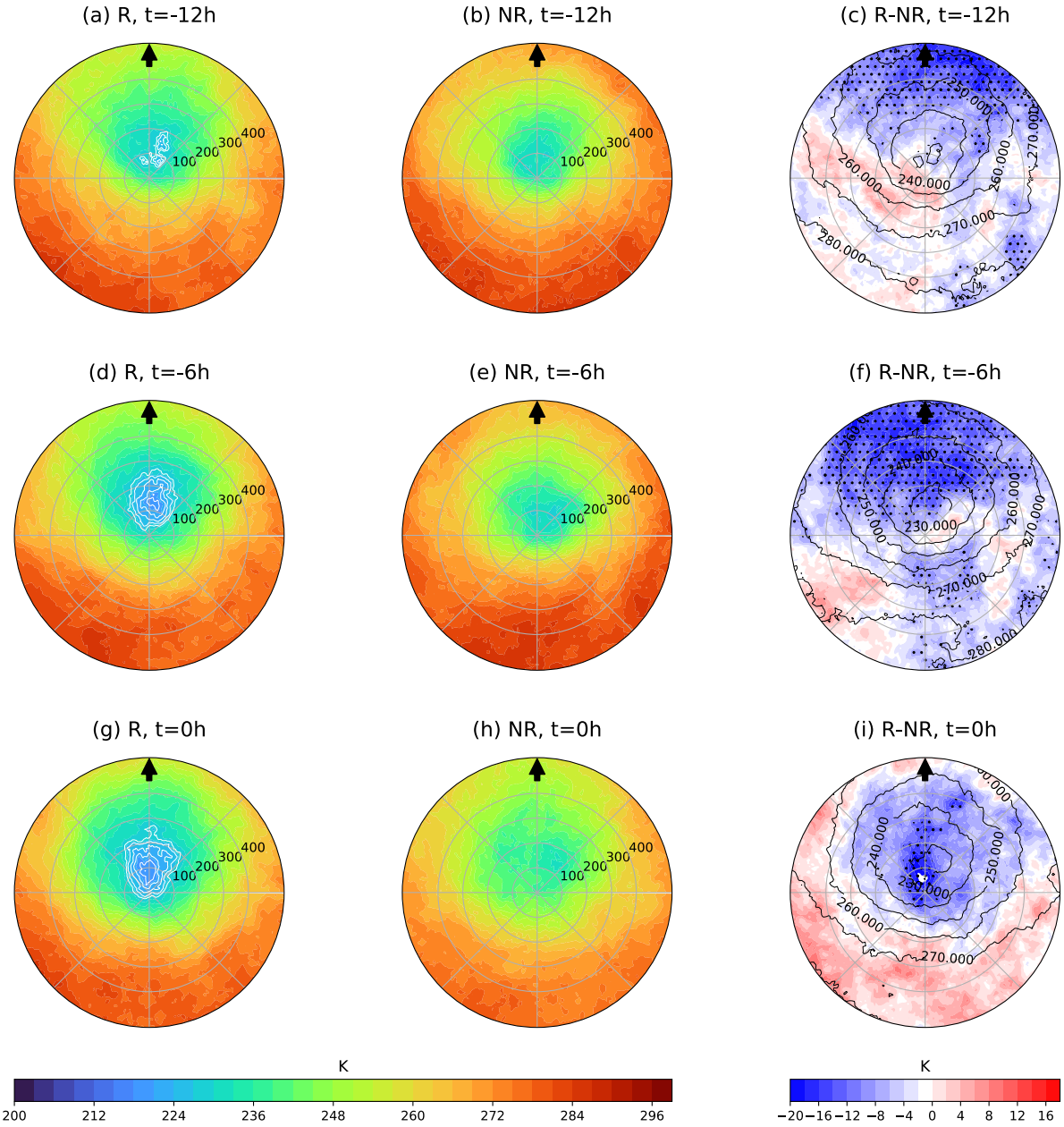

FIG.15. Similar to Fig. 7, except for the infrared brightness temperature (K). Brightness temperatures < 228 K are contoured in white.

4. Conclusions

This study aimed to identify the environmental conditions that favor the downshear reformation of tropical cyclones. North Atlantic tropical cyclones that reformed from 1998 to 2020 were identified from NHC discussions. Using an analog method, pairs of tropical cyclones that did and did not reform were matched with similar intensity, vertical wind shear, and maximum potential intensity.

Accepted for publication in *Monthly Weather Review*. DOI 10.1175/MWR-D-22-0251.1.

Reformation predominantly occurred in tropical storms under moderate shear within a few days after genesis. It is hypothesized that tropical cyclones are more prone to downshear reformation at this stage due to the circulation being more susceptible to environmental influences. These results are consistent with previous research (Nguyen and Molinari 2015; Chen et al. 2018b), and these factors are touched upon in forecast discussions; however, not every tropical storm under moderate vertical wind shear undergoes downshear reformation. The analog approach allowed us to systematically compare reformation and non-reformation cases to identify other factors that may favor the reformation of tropical cyclones.

A comparison of storm-centered, shear-relative composite fields revealed several factors that differ between reformation and non-reformation cases. The reformed storms were characterized by:

i. An asymmetric distribution of mid-to-upper tropospheric relative humidity with higher values downshear and lower values upshear.
ii. Greater low-level relative humidity over much of the inner 500 km.
iii. Larger CAPE and low-level θ_e right of shear.
iv. Larger surface latent heat fluxes left of shear and downshear due to stronger winds, associated with a stronger pressure gradient left of shear.

It is hypothesized that the increase in surface fluxes helps to increase the low-level θ_e and CAPE right of shear. These factors increase thermodynamic favorability, building a reservoir of potential energy. Downshear moistening aloft then minimizes dry air entrainment in convection. This combination promotes sustained convection downshear that deepens with time, leading to downshear reformation. Figure 16 shows a schematic diagram of select factors that favor downshear reformation.

Contrary to the reformation cases, the tropical cyclones that did not undergo downshear reformation had smaller surface fluxes left of shear; as a result, the low-level θ_e was not as large right of shear. In addition, the non-reformation storms were embedded in a drier lower-tropospheric environment. The non-reformed storms also had an asymmetric distribution of mid-to-upper tropospheric relative humidity with high values in downshear quadrants than in upshear quadrants. However, the downshear region was drier and the upshear region had higher relative humidity than the reformed tropical cyclones. In addition, contrary to the reformed tropical cyclones, the mid-tropospheric relative humidity decreased in the non-reformation

Accepted for publication in *Monthly Weather Review*. DOI 10.1175/MWR-D-22-0251.1.

composite with time in the upshear-left quadrant. This result is also in contrast to the evolution of mid-tropospheric relative humidity in successful cases of vortex alignment (Zawislak et al. 2016; Alvey et al. 2020). These factors are consistent with the weaker convection downshear, and deep convection confined closer to the center, favoring the continuation of the parent vortex as the dominant vortex.

We note some limitations of this study. First, it was not possible to identify the reformation cases objectively and the selection of cases was based on the forecaster's subjectivity. The 12-h track and intensity error analysis increased our confidence, but there is still uncertainty regarding the exact time of reformation and whether the non-reformation analog cases did not, in reality, undergo reformation. Second, the temporal and spatial resolution of the reanalysis data only allows broad-scale aspects of these tropical cyclones to be studied and not mesoscale processes involved in the reformation of tropical cyclones. Additionally, because of the temporal and spatial resolution of the reanalysis data, the reformation of the new center could not be resolved. Lastly, our sample was limited to North Atlantic tropical cyclones. Additional analysis of the reformation process in other basins should be conducted to check for consistency, as environmental characteristics may vary.

From a forecasting standpoint, recognizing patterns and factors that are favorable for downshear reformation (Fig. 16) may help forecasters to better anticipate downshear reformation or have greater confidence in a convection-allowing tropical cyclone model that simulates reformation. This study raises the possibility that there may be predictive skill in forecasting downshear reformation based on storm-scale and environmental cues.

Although more tropical cyclones within the reformation composite intensified, compared to the non-reformation composite, there was no definite relationship between reformation and subsequent intensity change. Questions considering the impact of the reformation in the vortex alignment process and its role in the intensification of tropical storms under moderate vertical wind shear remain, including how often the reformation successfully results in rapid intensification and how alignment is achieved: through the distinct redevelopment of the low-level vortex underneath the mid-level vortex or through a merger of the inner and parent vortices. Future work will involve high-resolution ensemble simulations that will allow the examination of the vortex structure, convective and mesoscale processes, and associated predictability issues involved in downshear reformation.

Accepted for publication in *Monthly Weather Review*. DOI 10.1175/MWR-D-22-0251.1.

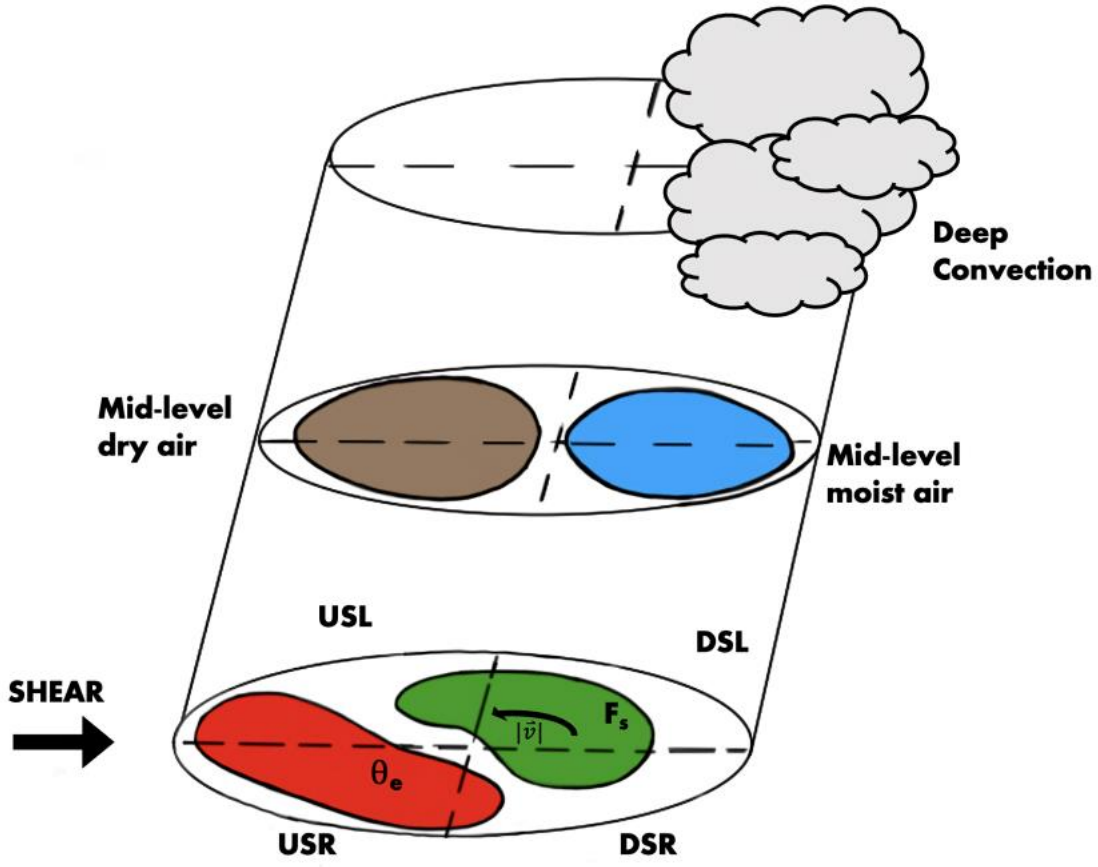

FIG. 16. Schematic diagram of the main factors this study identified as favoring downshear reformation in tropical cyclones. The green area represents larger surface latent heat fluxes (F_s), the arrow in this region represents stronger winds; the red area shows greater low-level equivalent potential temperature (θ_e). Mid-to-upper level dry and moist air are shown in the brown and blue areas, respectively. The clouds are downshear deep convection.

Acknowledgments

This research was supported by the University at Albany's Carson Carr Graduate Diversity Fellowship and NSF grants AGS-1748779 and AGS-2225604. We thank our reviewers for their comments and suggestions that improved our study.

Data Availability Statement

All data sets employed in this research are openly available. All ERA5 data is available from the Copernicus Climate Data Store (https://doi.org/10.24381/cds.bd0915c6; https://doi.org/10.24381/cds.adbb2d47). The GridSat-B1 data is publicly available from the National Centers for Environmental Information page. The data used to calculate the cost

Accepted for publication in *Monthly Weather Review*. DOI 10.1175/MWR-D-22-0251.1.

function (best track data and SHIPS diagnostic files) can be located in the NHC data archive and https://rammb.cira.colostate.edu/research/tropical_cyclones/ships/.

APPENDIX

Reformation Cases and Best Analog

Reformation Case	Time of Reformation	Analog, Non-reformation Case	Analog Time
Alberto 2006	2006-06-12 12 UTC	Leslie 2000	2000-10-06 06 UTC
Andrea 2013	2013-06-06 00 UTC	Delta 2005	2005-11-27 06 UTC
Arlene 1999	1999-06-15 12 UTC	Danny 2003	2003-07-17 06 UTC
Arlene 2005	2005-06-11 00 UTC	Sean 2011	2011-11-10 12 UTC
Beryl 2000	2000-08-14 12 UTC	Henri 2003	2003-09-05 12 UTC
Beryl 2006	2006-07-20 06 UTC	Cindy 2011	2011-07-20 18 UTC
Beta 2020	2020-09-20 18 UTC	Chris 2006	2006-08-02 12 UTC
Claudette 2003	2003-07-10 12 UTC	Josephine 2008	2008-09-04 18 UTC
Cristobal 2002	2002-08-07 00 UTC	Lorenzo 2013	2013-10-21 18 UTC
Cristobal 2008	2008-07-21 12 UTC	Hermine 2004	2004-08-30 00 UTC
Danny 2009	2009-08-27 00 UTC	Oscar 2012	2012-10-04 00 UTC
Debby 2000	2000-08-20 18 UTC	Alex 1998	1998-07-30 06 UTC
Dolly 2002	2002-09-03 12 UTC	Lisa 2004	2004-09-28 06 UTC
Don 2011	2011-07-29 00 UTC	Tropical Depression #15 (2019)	2019-10-15 00 UTC
Earl 2016	2016-08-03 06 UTC	Ivan 2004	2004-09-04 06 UTC
Edouard 2014	2014-09-13 00 UTC	Kyle 2008	2008-09-26 00 UTC
Emily 2005	2005-07-14 00 UTC	Maria 2005	2005-09-04 00 UTC
Emily 2011	2011-08-02 18 UTC	Stan 2005	2005-10-03 18 UTC
Erika 2009	2009-09-02 06 UTC	Emily 1999	1999-08-26 12 UTC
Erika 2015	2015-08-27 12 UTC	Igor 2010	2010-09-09 12 UTC
Erin 2007	2007-08-15 18 UTC	Jerry 2013	2013-09-29 12 UTC
Ernesto 2012	2012-08-06 12 UTC	Franklin 2005	2005-07-23 12 UTC
Eta 2020	2020-11-07 12 UTC	Tropical Depression #8 (2016)	2016-08-30 06 UTC
Felix 2001	2001-09-11 12 UTC	Kate 2003	2003-09-27 12 UTC
Florence 2006	2006-09-05 12 UTC	Tropical Depression #12 (1999)	1999-10-07 12 UTC

Accepted for publication in *Monthly Weather Review*. DOI 10.1175/MWR-D-22-0251.1.

Gabrielle 2001	2001-09-12 18 UTC	Ophelia 2005	2005-09-06 18 UTC
Gabrielle 2019	2019-09-07 18 UTC	Bertha 2014	2014-08-04 06 UTC
Gert 2005	2005-07-24 06 UTC	Dennis 2005	2005-07-05 06 UTC
Gustav 2008	2008-08-28 06 UTC	Irene 2011	2011-08-21 18 UTC
Hanna 2008	2008-09-04 00 UTC	Michael 2012	2012-09-06 00 UTC
Hanna 2020	2020-07-23 18 UTC	Floyd 1999	1999-09-08 06 UTC
Harvey 2011	2011-08-20 00 UTC	Bonnie 2004	2004-08-10 00 UTC
Harvey 2017	2017-08-24 06 UTC	Franklin 2017	2017-08-09 06 UTC
Helene 2018	2018-09-08 06 UTC	Helene 2006	2006-09-13 06 UTC
Humberto 2013	2013-09-17 06 UTC	Ingrid 2007	2007-09-15 00 UTC
Ian 2016	2016-09-14 12 UTC	Olga 2001	2001-11-25 00 UTC
Ida 2015	2015-09-22 12 UTC	Maria 2011	2011-09-11 06 UTC
Irene 2005	2005-08-07 06 UTC	Dean 2007	2007-08-14 00 UTC
Isaac 2012	2012-08-22 12 UTC	Karen 2019	2019-09-25 18 UTC
Isidore 2002	2002-09-18 18 UTC	Jerry 2019	2019-09-18 18 UTC
Jeanne 2004	2004-09-18 18 UTC	Grace 2015	2015-09-07 18 UTC
Jose 1999	1999-10-18 06 UTC	Wilma 2005	2005-10-16 06 UTC
Josephine 2020	2020-08-14 18 UTC	Dorian 2019	2019-08-25 06 UTC
Julia 2016	2016-09-15 12 UTC	Fiona 2016	2016-08-22 00 UTC
Karen 2007	2007-09-28 06 UTC	Odette 2003	2003-12-06 12 UTC
Karl 2016	2016-09-19 18 UTC	Erin 2019	2019-08-27 00 UTC
Leslie 2012	2012-09-03 00 UTC	Kirk 2018	2018-09-27 00 UTC
Lisa 2016	2016-09-20 18 UTC	Lorenzo 2001	2001-10-28 12 UTC
Michael 2018	2018-10-07 18 UTC	Harvey 1999	1999-09-19 18 UTC
Nadine 2012	2012-09-12 00 UTC	Earl 2010	2010-08-27 12 UTC
Noel 2007	2007-10-28 18 UTC	Kyle 2002	2002-10-10 00 UTC
Philippe 2011	2011-09-29 18 UTC	Isaac 2006	2006-09-29 06 UTC
Rafael 2012	2012-10-13 18 UTC	Gonzalo 2014	2014-10-13 00 UTC
Richard 2010	2010-10-22 18 UTC	Fiona 2010	2010-08-31 18 UTC
Sally 2020	2020-09-14 06 UTC	Florence 2000	2000-09-12 00 UTC
Tomas 2010	2010-10-30 00 UTC	Nate 2017	2017-10-06 18 UTC
Tropical Depression #14 (2002)	2002-10-15 18 UTC	Cristobal 2014	2014-08-24 12 UTC

Accepted for publication in *Monthly Weather Review*. DOI 10.1175/MWR-D-22-0251.1.

Tropical Depression #14 (2003)	2003-09-09 00 UTC	Helene 2012	2012-08-10 06 UTC
Zeta 2020	2020-10-25 06 UTC	Mitch 1998	1998-10-22 12 UTC

Table A1. Tropical cyclones that underwent downshear reformation used in this study, time of reformation, and best analog non-reformation case and time.

REFERENCES

Alland, J. J., B. H. Tang, K. L. Corbosiero, and G. H. Bryan, 2021a: Combined effects of midlevel dry air and vertical wind shear on tropical cyclone development. Part I: Downdraft ventilation. *J. Atmos. Sci.*, **78**, 763–782, https://doi.org/10.1175/JAS-D-20-0054.1.

——, ——, ——, and ——, 2021b: Combined efffects of midlevel dry air and vertical wind shear on tropical cyclone development. Part II: Radial ventilation. *J. Atmos. Sci.*, **78**, 783–796, https://doi.org/10.1175/JAS-D-20-0055.1.

Alvey, G. R., J. Zawislak, and E. Zipser, 2015: Precipitation properties observed during tropical cyclone intensity change. *Mon. Wea. Rev.*, **143**, 4476–4492, https://doi.org/10.1175/MWR-D-15-0065.1.

——, E. Zipser, and J. Zawislak, 2020: How does Hurricane Edouard (2014) evolve toward symmetry before rapid intensification? A high-resolution ensemble study. *J.Atmos. Sci*, **77**, 1329–1351, https://doi.org/10.1175/JAS-D-18-0355.1.

——, M. Fischer, P. Reasor, J. Zawislak, and R. Rogers, 2022: Observed processes underlying the favorable vortex repositioning early in the development of Hurricane Dorian (2019). *Mon. Wea. Rev.*, **150**, 193–213, https://doi.org/10.1175/MWR-D-21-0069.1.

Alvey III, G. R., and A. Hazelton, 2022: How do weak, misaligned tropical cyclones evolve toward alignment? A multi-case study ssing the hurricane analysis and forecast system. *J Geophys Res*, **127**, e2022JD037268, https://doi.org/10.1029/2022JD037268.

Black, M. L., J. F. Gamache, F. D. Marks, C. E. Samsury, and H. E. Willoughby, 2002: Eastern Pacific hurricanes Jimena of 1991 and Olivia of 1994: The effect of vertical shear on structure and intensity. *Mon. Wea. Rev.*, **130**, 2291–2312, https://doi.org/10.1175/1520-0493(2002)130<2291:EPHJOA>2.0.CO;2.

Cecil, D. J., 2007: Satellite-derived rain rates in vertically sheared tropical cyclones. *Geophys. Res. Lett.*, **34**, https://doi.org/10.1029/2006GL027942.

Chen, B.-F., C. A. Davis, and Y.-H. Kuo, 2018a: Effects of low-level flow orientation and vertical shear on the structure and intensity of tropical cyclones. *Mon. Wea. Rev.*, **146**, 2447–2467, https://doi.org/10.1175/MWR-D-17-0379.1.

Accepted for publication in *Monthly Weather Review*. DOI 10.1175/MWR-D-22-0251.1.

——, ——, and ——, 2019a: An idealized numerical study of shear-relative low-level mean flow on tropical cyclone intensity and size. *J. Atmos. Sci.*, **76**, 2309–2334, https://doi.org/10.1175/JAS-D-18-0315.1.

——, ——, and ——, 2021a: Examination of the combined effect of deep-layer vertical shear direction and lower-tropospheric mean flow on tropical cyclone intensity and size based on the ERA5 reanalysis. *Mon. Wea. Rev.*, **149**, 4057–4076, https://doi.org/10.1175/MWR-D-21-0120.1.

Chen, S. S., J. A. Knaff, and F. D. Marks, 2006: Effects of vertical wind shear and storm motion on tropical cyclone rainfall asymmetries deduced from TRMM. *Mon. Wea. Rev.*, **134**, 3190–3208, https://doi.org/10.1175/MWR3245.1.

Chen, X., Y. Wang, J. Fang, and M. Xue, 2018b: A numerical study on rapid intensification of Typhoon Vicente (2012) in the South China Sea. Part II: Roles of inner-core processes. *J. Atmos. Sci.*, **75**, 235–255, https://doi.org/10.1175/JAS-D-17-0129.1.

——, J. A. Zhang, and F. D. Marks, 2019b: A thermodynamic pathway leading to rapid intensification of tropical cyclones in shear. *Geophys. Res. Lett.*, **46**, 9241–9251, https://doi.org/10.1029/2019GL083667.

——, J.-F. Gu, J. A. Zhang, F. D. Marks, R. F. Rogers, and J. J. Cione, 2021b: Boundary layer recovery and precipitation symmetrization preceding rapid intensification of tropical cyclones under shear. *J. Atmos. Sci.*, **78**, 1523–1544, https://doi.org/10.1175/JAS-D-20-0252.1.

Corbosiero, K. L., and J. Molinari, 2002: The effects of vertical wind shear on the distribution of convection in tropical cyclones. *Mon. Wea. Rev.*, **130**, 2110–2123, https://doi.org/10.1175/1520-0493(2002)130<2110:TEOVWS>2.0.CO;2.

Davis, C. A., S. C. Jones, and M. Riemer, 2008: Hurricane vortex dynamics during Atlantic extratropical transition. *J.Atmos. Sci*, **65**, 714–736, https://doi.org/10.1175/2007JAS2488.1.

DeHart, J. C., R. A. Houze, and R. F. Rogers, 2014: Quadrant distribution of tropical cyclone inner-core kinematics in relation to environmental shear. *J. Atmos. Sci.*, **71**, 2713–2732, https://doi.org/10.1175/JAS-D-13-0298.1.

DeMaria, M., 1996: The effect of vertical shear on tropical cyclone intensity change. *J. Atmos. Sci.*, **53**, 2076–2088, https://doi.org/10.1175/1520-0469(1996)053<2076:TEOVSO>2.0.CO;2.

——, and J. Kaplan, 1994: A statistical hurricane intensity prediction scheme (SHIPS) for the Atlantic Basin. *Wea. Forecasting*, **9**, 209–220, https://doi.org/10.1175/1520-0434(1994)009<0209:ASHIPS>2.0.CO;2.

——, M. Mainelli, L. K. Shay, J. A. Knaff, and J. Kaplan, 2005: Further improvements to the statistical hurricane intensity prediction scheme (SHIPS). *Wea. Forecasting*, **20**, 531–543, https://doi.org/10.1175/WAF862.1.

Accepted for publication in *Monthly Weather Review*. DOI 10.1175/MWR-D-22-0251.1.

Fischer, M. S., B. H. Tang, and K. L. Corbosiero, 2019: A climatological analysis of tropical cyclone rapid intensification in environments of upper-tropospheric troughs. *Mon. Wea. Rev.*, **147**, 3693–3719, https://doi.org/10.1175/MWR-D-19-0013.1.

Galarneau, T. J., and C. A. Davis, 2013: Diagnosing forecast errors in tropical cyclone motion. *Mon. Wea. Rev.*, **141**, 405–430, https://doi.org/10.1175/MWR-D-12-00071.1.

Halperin, D. J., and R. D. Torn, 2018: Diagnosing conditions associated with large intensity forecast errors in the Hurricane Weather Research and Forecasting (HWRF) model. *Wea. Forecasting*, **33**, 239–266, https://doi.org/10.1175/WAF-D-17-0077.1.

Hersbach, H., and Coauthors, 2020: The ERA5 global reanalysis. *Q. J. R. Meteorol. Soc.*, **146**, 1999–2049, https://doi.org/10.1002/qj.3803.

Jones, S. C., 1995: The evolution of vortices in vertical shear. I: Initially barotropic vortices. *Q. J. R. Meteorol. Soc.*, **121**, 821–851, https://doi.org/10.1002/qj.49712152406.

Kaplan, J., M. DeMaria, and J. A. Knaff, 2010: A revised tropical cyclone rapid intensification index for the Atlantic and Eastern North Pacific basins. *Wea. Forecasting*, **25**, 220–241, https://doi.org/10.1175/2009WAF2222280.1.

Knapp, K. R., and Coauthors, 2011: Globally gridded satellite observations for climate studies. *Bull. Amer. Mteor. Soc.*, **92**, 893–907, https://doi.org/10.1175/2011BAMS3039.1.

Landsea, C. W., and J. L. Franklin, 2013: Atlantic hurricane database uncertainty and presentation of a new database format. *Mon. Wea. Rev.*, **141**, 3576–3592, https://doi.org/10.1175/MWR-D-12-00254.1.

Molinari, J., and D. Vollaro, 2010: Rapid intensification of a sheared tropical storm. *Mon. Wea. Rev.*, **138**, 3869–3885, https://doi.org/10.1175/2010MWR3378.1.

——, ——, and K. L. Corbosiero, 2004: Tropical cyclone formation in a sheared environment: A case study. *J. Atmos. Sci.*, **61**, 2493–2509, https://doi.org/10.1175/JAS3291.1.

——, P. Dodge, D. Vollaro, K. L. Corbosiero, and F. Marks, 2006: Mesoscale aspects of the downshear reformation of a tropical cyclone. *J. Atmos. Sci.*, **63**, 341–354, https://doi.org/10.1175/JAS3591.1.

——, D. M. Romps, D. Vollaro, and L. Nguyen, 2012: CAPE in Tropical Cyclones. *J. Atmos. Sci.*, **69**, 2452–2463, https://doi.org/10.1175/JAS-D-11-0254.1.

Nguyen, L. T., and J. Molinari, 2015: Simulation of the downshear reformation of a tropical cyclone. *J. Atmos. Sci.*, **72**, 4529–4551, https://doi.org/10.1175/JAS-D-15-0036.1.

——, R. Rogers, J. Zawislak, and J. A. Zhang, 2019: Assessing the influence of convective downdrafts and surface enthalpy fluxes on tropical cyclone intensity change in moderate vertical wind shear. *Mon. Wea. Rev.*, **147**, 3519–3534, https://doi.org/10.1175/MWR-D-18-0461.1.

Accepted for publication in *Monthly Weather Review*. DOI 10.1175/MWR-D-22-0251.1.

Rappin, E. D., and D. S. Nolan, 2012: The effect of vertical shear orientation on tropical cyclogenesis. *Q. J. R. Meteorol. Soc.*, **138**, 1035–1054, https://doi.org/10.1002/qj.977.

Raymond, D. J., S. Gjorgjievska, S. Sessions, and Ž. Fuchs, 2014: Tropical cyclogenesis and mid-level vorticity. *Aust. Meteor. and Ocean. J.*, **64**, 11–25, https://doi.org/10.1071/es14003.

Reasor, P. D., M. T. Montgomery, and L. D. Grasso, 2004: A new look at the problem of tropical cyclones in vertical shear flow: Vortex resiliency. *J. Atmos. Sci.*, **61**, 3–22, https://doi.org/10.1175/1520-0469(2004)061<0003:ANLATP>2.0.CO;2.

——, R. Rogers, and S. Lorsolo, 2013: Environmental flow impacts on tropical cyclone structure diagnosed from airborne doppler radar composites. *Mon. Wea. Rev.*, **141**, 2949–2969, https://doi.org/10.1175/MWR-D-12-00334.1.

Richardson, J. C., R. D. Torn, and B. H. Tang, 2022: An analog comparison between rapidly and slowly intensifying tropical cyclones. *Mon. Wea. Rev.*, **150**, 2139–2156, https://doi.org/10.1175/MWR-D-21-0260.1.

Riemer, M., M. T. Montgomery, and M. E. Nicholls, 2010: A new paradigm for intensity modification of tropical cyclones: thermodynamic impact of vertical wind shear on the inflow layer. *Atmos. Chem. Phys.*, 26.

Rios-Berrios, R., and R. D. Torn, 2017: Climatological analysis of tropical cyclone intensity changes under moderate vertical wind shear. *Mon. Wea. Rev.*, **145**, 1717–1738, https://doi.org/10.1175/MWR-D-16-0350.1.

——, ——, and C. A. Davis, 2016: An ensemble approach to investigate tropical cyclone intensification in sheared environments. Part I: Katia (2011). *J. Atmos. Sci.*, **73**, 71–93, https://doi.org/10.1175/JAS-D-15-0052.1.

Rogers, R. F., P. D. Reasor, J. A. Zawislak, and L. T. Nguyen, 2020: Precipitation processes and vortex alignment during the intensification of a weak tropical cyclone in moderate vertical shear. *Mon. Wea. Rev.*, **148**, 1899–1929, https://doi.org/10.1175/MWR-D-19-0315.1.

Ryglicki, D. R., J. D. Doyle, Y. Jin, D. Hodyss, and J. H. Cossuth, 2018: The unexpected rapid intensification of tropical cyclones in moderate vertical wind shear. Part II: Vortex tilt. *Mon. Wea. Rev.*, **146**, 3801–3825, https://doi.org/10.1175/MWR-D-18-0021.1.

Schecter, D. A., and K. Menelaou, 2020: Development of a misaligned tropical cyclone. *J. Atmos. Sci.*, **77**, 79–111, https://doi.org/10.1175/JAS-D-19-0074.1.

Shapiro, L. J., and H. E. Willoughby, 1982: The response of balanced hurricanes to local sources of heat and momentum. *J. Atmos. Sci.*, **39**, 378–394, https://doi.org/10.1175/1520-0469(1982)039<0378:TROBHT>2.0.CO;2.

Stone, Ž., G. R. Alvey, J. P. Dunion, M. S. Fischer, D. J. Raymond, R. F. Rogers, S. Sentić, and J. Zawislak, 2023: Thermodynamic contribution to vortex alignment and rapid

Accepted for publication in *Monthly Weather Review*. DOI 10.1175/MWR-D-22-0251.1.

intensification of hurricane Sally (2020). *Mon. Wea. Rev.*, **151**, 931–951, https://doi.org/10.1175/MWR-D-22-0201.1.

Tao, D., and F. Zhang, 2014: Effect of environmental shear, sea-surface temperature, and ambient moisture on the formation and predictability of tropical cyclones: An ensemble-mean perspective. *J. Adv. Model. Earth Syst.*, **6**, 384–404, https://doi.org/10.1002/2014MS000314.

Wang, Z., 2018: What is the key feature of convection leading up to tropical cyclone formation? *J. Atmos. Sci.*, **75**, 1609–1629, https://doi.org/10.1175/JAS-D-17-0131.1.

Yu, C., B. H. Tang, and R. G. Fovell, 2023: Tropical cyclone tilt and precession in moderate shear: Precession hiatus in a critical shear regime. *J. Atmos. Sci.*, **80**, 909–932, https://doi.org/10.1175/JAS-D-22-0200.1.

Zawislak, J., H. Jiang, G. R. Alvey, E. J. Zipser, R. F. Rogers, J. A. Zhang, and S. N. Stevenson, 2016: Observations of the structure and evolution of Hurricane Edouard (2014) during intensity change. Part I: Relationship between the thermodynamic structure and precipitation. *Mon. Wea. Rev.*, **144**, 3333–3354, https://doi.org/10.1175/MWR-D-16-0018.1.

Zhang, J. A., R. F. Rogers, P. D. Reasor, E. W. Uhlhorn, and F. D. Marks, 2013: Asymmetric hurricane boundary layer structure from dropsonde composites in relation to the environmental vertical wind shear. *Mon. Wea. Rev.*, **141**, 3968–3984, https://doi.org/10.1175/MWR-D-12-00335.1.

Accepted for publication in *Monthly Weather Review*. DOI 10.1175/MWR-D-22-0251.1.